



<https://theses.gla.ac.uk/>

Theses Digitisation:

<https://www.gla.ac.uk/myglasgow/research/enlighten/theses/digitisation/>

This is a digitised version of the original print thesis.

Copyright and moral rights for this work are retained by the author

A copy can be downloaded for personal non-commercial research or study,
without prior permission or charge

This work cannot be reproduced or quoted extensively from without first
obtaining permission in writing from the author

The content must not be changed in any way or sold commercially in any
format or medium without the formal permission of the author

When referring to this work, full bibliographic details including the author,
title, awarding institution and date of the thesis must be given

Enlighten: Theses

<https://theses.gla.ac.uk/>
research-enlighten@glasgow.ac.uk

REDUCTION OF LEADING EDGE TEMPERATURES
DURING HIGH SPEED FLIGHT.

William M.B. Steele, B.Sc.

Thesis submitted for the degree of M.Sc.

To the Faculty of Engineering,

The University of Glasgow.

Department of Aeronautics and
Fluid Mechanics.

April, 1973.

ProQuest Number: 10662701

All rights reserved

INFORMATION TO ALL USERS

The quality of this reproduction is dependent upon the quality of the copy submitted.

In the unlikely event that the author did not send a complete manuscript and there are missing pages, these will be noted. Also, if material had to be removed, a note will indicate the deletion.



ProQuest 10662701

Published by ProQuest LLC (2017). Copyright of the Dissertation is held by the Author.

All rights reserved.

This work is protected against unauthorized copying under Title 17, United States Code
Microform Edition © ProQuest LLC.

ProQuest LLC.
789 East Eisenhower Parkway
P.O. Box 1346
Ann Arbor, MI 48106 – 1346

ACKNOWLEDGEMENTS.

The work embodied in this thesis has been carried out with the financial assistance of a Ministry of Technology contract, No. FD/48/09/SRA.

The author wishes to acknowledge his indebtedness to Professor T.R.F. Nonweiler and Dr. H.Y. Wong for their most valuable advice and guidance in pursuing this work and would like to sincerely thank them. He also acknowledges with gratitude the assistance provided by all those with whom he has come in contact during the course of his research.

LIST OF CONTENTS

| | |
|--|-----|
| List of Figures | i |
| List of Tables | iii |
| Nomenclature | iv |
| Summary | v |
| <u>Chapter I</u> | |
| Introduction | 1 |
| <u>Chapter II</u> | |
| Survey of Previous Work | 5 |
| <u>Chapter III</u> | |
| Theoretical and Experimental Investigation of a Leading Edge with a Highly Conducting Nose | 16 |
| 3.1 Introduction | 16 |
| 3.2 Theoretical Analysis of the Composite Leading Edge | 17 |
| 3.2.1 Derivation of the Heat Conduction Equation | 17 |
| 3.2.2 Modification of the heat conduction equation to deal with the variation of thermal properties of the composite materials | 20 |
| 3.2.3 Discussion of Theoretical Results | 23 |
| 3.3 Experimental Analysis of the Composite Leading Edge | 29 |
| 3.3.1 Simulation of Aerodynamic Heating | 29 |
| 3.3.2 Test Models | 31 |
| 3.3.3 Method of Bonding Copper Nose to Stainless Steel Body | 34 |
| 3.3.4 Treatment of the Model Surface exposed to Radiation | 35 |
| 3.3.5 Apparatus and Experimental Procedure | 36 |

| | | |
|-------|---|----|
| 3.3.6 | Experimental Errors | 40 |
| 3.3.7 | Discussion and Comparison of Theory with Experiment | 41 |

Chapter IV

| | | |
|-------|---|----|
| | Investigation of the effect of the shape of the Leading Edge | 47 |
| 4.1 | Introduction | 47 |
| 4.2 | Theoretical Analysis of the Leading Edge | 48 |
| 4.3 | Theoretical Results and Discussion | 51 |
| 4.4 | Experimental Analysis of an Optimised Shape Leading Edge | 59 |
| 4.4.1 | Test Model | 59 |
| 4.4.2 | Experimental Procedure | 63 |
| 4.5 | Discussion | 64 |

Chapter V

| | | |
|------------|--|----|
| | Conclusions and General Discussions | 67 |
| Appendix A | Derivation of the Heat Conduction Equation in a Finite Differences Form | 72 |
| Appendix B | ALGOL - 60 Computer Program | 77 |
| References | | 91 |

List of Figures

| Figure Nos. | | Page |
|-------------|---|------|
| 2.1 | Comparison between temperature distributions for different methods of expressing thickness variations (slab) | 13 |
| 2.2. | Comparison between temperature distributions for different methods of expressing thickness variations (trapezoidal) | 14. |
| 2.3 | Comparison between temperature distributions for different methods of expressing thickness variations (wedge) | 15 |
| 3.2.2 | Representation of a copper-stainless steel leading edge | 20 |
| 3.2.3.1 | Theoretical comparisons for composite leading edge (slab) | 24 |
| 3.2.3.2 | Theoretical comparisons for composite leading edge (trapezoidal) | 25 |
| 3.2.3.3 | Theoretical comparisons for composite leading edge (wedge) | 26 |
| 3.2.3.4. | Graph % Reduction in Nose Temperature vs. Convective Heat Input | 29 |
| 3.3.2 | Typical copper-stainless steel test model | 33 |
| 3.3.5.1 | General Layout of Experimental Apparatus | 37 |

| | | |
|-----------|---|----|
| 3.3.7.1 | Experimental Results for Composite Model 1 | 42 |
| 3.3.7.2 | " 2 | 43 |
| 3.3.7.3 | " 3 | 44 |
| 3.3.7.4 | " 4 | 45 |
| 4.2.1 | Plot of $H(L) / I_Q(L)$ vs. $\alpha L / T_L$ | 52 |
| 4.3.1 | Theoretical comparison between optimised shapes and general simple shapes for $Q_0 = 1250 \text{ W/m}^{3/2}$ | 54 |
| 4.3.2 | Theoretical comparison between optimised shapes and general simple shapes for $Q_0 = 5000 \text{ W/m}^{3/2}$ | 55 |
| 4.3.3 | Theoretical comparison between optimised shapes and general simple shapes for $Q_0 = 10000 \text{ W/m}^{3/2}$ | 56 |
| 4.3.4 | Comparison with slab model of Figure 2.1 for model which has a linear, but not optimised temperature distribution | 58 |
| 4.4.1 (a) | Theoretical shape of experimental model | 62 |
| 4.4.1 (b) | Actual " " " | 62 |
| 4.5.1 | Comparison between Experimental Results and Predicted Temperature Distribution | 66 |

List of Tables.

| <u>Table Nos.</u> | | <u>Page</u> |
|-------------------|--|-------------|
| 3.3.2 | Test Models | 32 |
| 3.3.5.1 | Experimental Results for Copper-Stainless Steel Models | 39 |
| 4.4.1 | Thickness Distribution for Experimental Model | 61 |
| 4.4.2 | Experimental Results and Comparison with Predicted values | 65 |

NOMENCLATURE

Principal Symbols used throughout this Thesis

| SYMBOL | | UNITS |
|------------|---|-----------------|
| k | Thermal conductivity of the material | $W/m^{\circ}K$ |
| t | thickness of the conducting material | m |
| ϵ | co-efficient of emissivity | |
| σ | Stefan - Boltzmann Constant - $5.67 \times 10^{-8} W/m^2 \cdot ^{\circ}K^4$ | |
| T | Temperature | $^{\circ}K$ |
| x | Distance from the leading edge | m |
| x_0 | Constant - 0.004191m | |
| Q | Convective Heat Input | W/m^2 |
| Q_0 | Convective heat input constant | $W/m^{3/2}$ |
| L | Length of conducting surface | m |
| R | Junction resistance to heat flow | $m^2 \cdot K/W$ |
| l | Length of constituent material of composite leading edge | m |
| α | Variation of temperature with distance from leading edge | $^{\circ}K/m$ |

Subscripts

| | |
|---|---|
| 1 | refers to copper portion of leading edge, chapter III |
| 2 | " " stainless steel portion of leading edge |
| o | values of parameters at $x = 0$ |
| L | " " " " $x = L$ |

SUMMARY

It has already been shown that by taking into consideration the conducting power of the leading edge material, nose temperatures are substantially reduced compared to the case where aerodynamic heating is balanced by radiation alone. The leading edge is envisaged as a "conducting plate" and the heat transfer equations formulated. This investigation is concerned with two particular methods of reducing leading edge temperatures by increasing the conducting power of the leading edge.

The first involves manufacturing a leading edge consisting of a basic structural material on to which is bonded a nose of highly conducting material. The main problem which arises is that a thermal resistance may be set up across the interface of the two structural materials and it is possible that the reduction gained in nose temperature will be offset by this thermal resistance. Steady state heat transfer equations are set up to allow for the variation in material properties. Experimentation is carried out to determine the junction thermal resistance, which cannot be obtained analytically, and to investigate the accuracy of the results predicted by the solution of the heat transfer equations. Models of simple shapes, are manufactured from copper and stainless steel to represent the leading edge and are subjected to simulated aerodynamic heating.

The object of the other part of the investigation is to find the material distribution for a leading edge such that it has

a minimum nose temperature for the amount of material available and a linear temperature distribution over its length. Previous investigations have been concerned mainly with relatively simple leading edge shapes. By taking the temperature distribution as linear a stress free leading edge is obtained and the analysis of the thickness distribution is considerably simplified since the heat transfer equation becomes directly integrable. A model was manufactured on the basis of the analysis and subjected to simulated aerodynamic heating to provide a comparison with the predicted results.

CHAPTER I

INTRODUCTION

The effects of aerodynamic heating on the structural integrity of high supersonic aircraft are well known. In particular the parts of the aircraft situated at the forward position, such as the nose and leading edge, are subjected to the most severe heating and become the most critical parts in the design of such aircraft.

Temperatures at these regions under aerodynamic heating may easily exceed the limits of the maximum temperature tolerable to any available structural materials if provision is not made for removal of the absorbed heat. These limits must include considerations for the preservation of strength and rigidity of the aircraft structure at all time during flight. Considerations of the temperature limits may even be extended to cover thermal fatigue if that should become one of the design requirements. As far as the design problem caused by aerodynamic heating is concerned, the forward parts of a high speed vehicle require special attention. The present investigation is directed towards the heating of the leading edge, with the object of alleviating the leading edge temperature of an aircraft flying at hypersonic speed.

One method of heat dissipation is by radiation from the surface of the aircraft. Radiation equilibrium temperature is

defined as the temperature, at which heat input to, is in equilibrium with heat dissipation by radiation from, the surface.

At the leading edge, which usually suffers from the highest heat input rate, the radiation equilibrium temperature can reach an unbelievably high value, whereas away from the leading edge, radiation equilibrium temperatures are relatively low not to cause any immediate concern. This is due to the fact that the heat input rate downstream from the leading edge is relatively low, compared to those at the leading edge. But the existence of radiation equilibrium temperatures in the vicinity of a leading edge is very doubtful, for if it were true there would also exist in this region a very high temperature gradient along the skin. The presence of a temperature gradient in a solid material will inevitably induce conductive heat flow in the material unless the material is a perfect insulator which we know does not exist in practice. Heat flow by conduction from higher to lower temperature levels must render some help towards reducing the nose temperature at the leading edge, for the higher the temperature gradient, the more effective will be the conduction of heat from the nose downstream. It is evident, therefore, to accept the presence of sufficient conducting material at the leading edge as being a fictitious heat pump for the alleviation of nose temperature. The power of such a heat pump may be looked upon as being in direct proportion to the product of the thermal conductivity and the volume of material employed in this region.

Ideally we prefer a large volume of highly conducting material to be situated at the nose. Often, however, the nose space of a leading edge is rather restricted to allow a large quantity of

material to be concentrated there; there is also the unnecessary weight penalty to be borne in mind. If the shape of the leading edge and hence the volume of space available is already specified, an increase in the material conducting power can only be realised by an increase in thermal conductivity of the material. One possible method of achieving this is by inserting rods of highly conducting material, in a chordwise direction, in the leading edge structure. These rods will provide channels for heat flow downstream, away from the nose. Problems, however, arise in constructing such a system. The thermal expansions of the two materials at the working temperature may differ, which may, either, introduce thermal stress in this already highly heated and highly strained region or, create unnecessarily high thermal contact resistance between the rods and the main body to deprive them of their potential as heat channels; the spacing of the rods would be important, since, the wider the spacing the greater would be the variation in temperature along the leading edge; the rods would have to be manufactured to very accurate limits since they would probably be inserted into the leading edge after its construction. Taking these drawbacks into consideration it would appear more practical (and simpler) to construct a leading edge on to which was bonded a nose of a highly conducting material; however, it is possible that a thermal resistance would be set up at the joint of the two materials. The problem which arises is whether the thermal resistance produced at the joint will offset the advantage of having a highly conducting nose.

Another aspect of this investigation concerns the shape of the leading edge. Previous investigations have, in the main, been limited to the analysis of, and experimentation with, leading edge shapes, which are uncomplicated to manufacture, such as slabs, trapezoidals and wedges; the investigations concerning these simple shapes are discussed, in more detail, in Chapter 2.

If the cross - sectional area, and consequently the volume of material at the leading edge, are specified it should be possible, by varying the thickness distribution of the material, to render the nose temperature a minimum for that specified area and heat input. In addition, the thickness distribution of the material could be arranged in such a way as to provide a prescribed temperature variation over the leading edge. We have investigated the evaluation of a thickness distribution of a leading edge which would have a linear temperature distribution and minimum nose temperature for a prescribed quantity of leading edge material and heat input. A temperature distribution with uniform gradient was chosen since it produces zero thermal stresses, and also considerably simplifies the analysis of the thickness distribution. Despite experimental limitations, and problem of manufacture, a leading edge, which fulfills the above conditions, was constructed and tested, to provide a comparison with the theoretical analysis.

CHAPTER II.SURVEY OF PREVIOUS WORK.

Previous investigations, which have been concerned with reducing leading edge temperatures during high speed flight, have tended to ignore the material properties of the leading edge. These investigations have assumed that the values of leading edge temperatures are close to radiation equilibrium values and that any means of reducing temperatures is by employing artificial cooling. One particular property which is likely to be a significant temperature reducing factor, is the conducting power of the leading edge material; by considering this and other factors, such as the shape of the leading edge, it may be possible to design a leading edge whose nose temperature is reduced to a level which is acceptable to presently known materials, and consequently does not require cooling.

It is convenient at this point, to mention briefly some possible cooling methods. The heat sink method requires a sufficient amount of material at the leading edge to absorb the heat input; however the amount of material which could be added is limited by the space available and the weight consideration for the vehicle. Mass transfer cooling involves injecting high specific heat gas or liquid into the boundary layer through openings in the surface of the leading edge structure. The development of the boundary layer and consequently the heat transfer rate to the body is greatly affected by the introduction of this foreign fluid; in addition, heat

may be absorbed by a change of phase of the coolant, e.g. sublimation or evaporation. The disadvantages of mass transfer cooling are that the system requires pumps, coolant storage tanks, pressure regulators, etc. The construction and maintenance of a porous leading edge surface would present serious difficulties. If the vehicle depended solely on mass transfer cooling as a method of heat removal then the system would have to be very reliable. Ablation cooling is the process of gradual loss of material at the surface of a vehicle exposed to severe rates of heating. The material either melts, vaporises or decomposes chemically, and in so doing absorbs heat, and then flows away into the boundary layer. Gasses are normally produced during ablation and, once produced, they force their way into the boundary layer and cause a blockage of heat transfer. An attractive feature of ablation as a means of heat removal is that the rate of melting or vaporisation adjusts itself automatically to the rate at which heat is being transferred to the surface. The heat pipe ¹ is a structure which, by virtue of its internal construction, is capable of transferring heat at high rates over appreciable distances while remaining relatively isothermal and without the need for external pumping. It is envisaged that the heat pipe would form an integral part of the leading edge and would extend into the adjacent portion of the downstream wing structure. Heat would be transported through the heat pipe from the leading edge to the downstream section and then radiated through the surface to the environment.

We, will, in the main, be concerned only with investigations which have considered the effects of leading edge design, without cooling, and, in particular, those which deal with the conducting ability of the leading edge material.

Nonweiler² was one of the first to recognize the potential available for reducing leading edge temperatures by employing conducting materials at the critical parts of high speed vehicles. More recently³ the same author has discussed the problems involved in designing manned high speed vehicles. These are the effect on the occupant of acceleration and retardation and the temperature of the environment. We are concerned only with the temperature aspects. Nonweiler, by considering a very simple representation of a manned vehicle, produces figures for leading edge temperatures and also the thermal stresses involved. The leading edge temperatures are found to be just beyond the range of known materials, but this problem could be significantly reduced for only a slight reduction in temperatures. Some suggestions on how to achieve this reduction are made e.g. by adding a projection of conducting material to the leading edge.

Naysmith and Woodley⁴ have produced radiation equilibrium temperatures for aircraft at varying hypersonic speeds and varying altitudes. These temperatures can be taken as maximum possible surface temperatures, since they are calculated on the basis of zero heat conduction in the body and the aerodynamic heat input to the surface is balanced exactly by radiation emitted from the surface.

As can be seen from the figures produced, the equilibrium temperatures at the leading edge are extremely high. Obviously, in practice, the body could not be a perfect insulator and heat conduction exists in the material where there is a temperature gradient.

Capey⁵ investigated the effect of material thermal conduction, as well as radiation, on the leading edges of vehicles in high speed flight. The variation of surface temperature with distance from the leading edge is calculated for two cases; firstly, the leading edge is assumed to be a perfect insulator and secondly, the leading edge is constructed of a conducting material or contains an insert of conducting material. Some consideration is also given to the shape of the leading edge, relating the variation of skin temperature with leading edge nose radius. The results for the insulated case are selected from the results produced by Naysmith and Woodley. For the conducting leading edge the heat conduction equation is solved by a finite differences method. It is assumed that there is no temperature variation normal to the surface of each finite element. The temperature distribution is obtained by equating to zero the total heat input into each segment, which is composed of aerodynamic, radiative and conductive terms.

The conclusions of this report were that a leading edge constructed of non - conducting material would suffer severely high surface equilibrium temperatures, whereas a leading edge of conducting material, subjected to the same heat input rates would have considerably reduced nose temperatures.

Nonweiler, Wong and Aggarwal^{6,7} investigated the effect of material thermal conduction on the leading edge heating of a high speed aircraft wing. An aircraft wing can be a very complex structure and when it is subjected to aerodynamic heating difficulties arise in calculating the temperature distribution produced. To overcome these difficulties Nonweiler, Wong and Aggarwal envisaged the leading edge of the wing as a conducting plate and then put forward a suitable theory. Mathematical analyses were then carried out, for simple representations of a leading edge, with the aid of a digital computer. The flow at the leading edge is taken to be laminar and aerodynamic heating originating from the boundary layer is assumed proportional to $x^{-\frac{1}{2}}$ where x is the distance from the leading edge. Similarity relations are also produced which show how experimentation at laboratory restricted temperature levels can be scaled up to provide information of practical value. The theoretical results gained from the conducting plate theory are compared experimentally with three simple shapes of leading edge - a slab, wedge and trapezoidal. In these experiments aerodynamic heating is simulated by radiation provided by the combination of an electric filament heater and a reflector^{8,9} which is specially designed to give a radiation intensity distribution proportional to $x^{-\frac{1}{2}}$. Very good agreement was shown to exist between theoretical and experimental results.

The conclusion reached by Nonweiler, Wong and Aggarwal was, in agreement with Capey, that heat conduction at the leading edge played a predominant role in reducing nose temperatures.

Aggarwal¹⁰ reproduces the results of reference 6 in greater detail. An, in detail, explanation of the method of overcoming the singularity in the laminar heat transfer expression at the leading edge is given. This problem was discussed briefly in reference 6. The heat input distribution, from the boundary layer to the leading edge, is taken as being proportional to $x^{-\frac{1}{2}}$; as, is obvious, the heating rates at the nose i.e. where $x = 0$ would become infinite. Consequently it would be impossible to produce experimental results for comparison with theoretical results. The problem is overcome by the introduction of a constant x_0 , which is small in comparison with the length of the experimental model; the heat input distribution now becomes proportional to $(x + x_0)^{-\frac{1}{2}}$. As can be seen the heating rates at the leading edge are now finite without causing significant change in the heat input expression. Experimental support for the choice of value x_0 is provided. Three different analytical methods of solving the equation obtained from the conducting plate theory, have been studied, one of which was extended to deal with the two-dimensional case. A solution of the heat conduction equation for a plane delta wing shape was obtained. The effects of varying the span and sweep - back angle on the temperature distribution and, in particular, the magnitude of nose temperature are examined. An account of the development of a simple wire heater, to simulate aerodynamic heating over the delta wing model, is given.

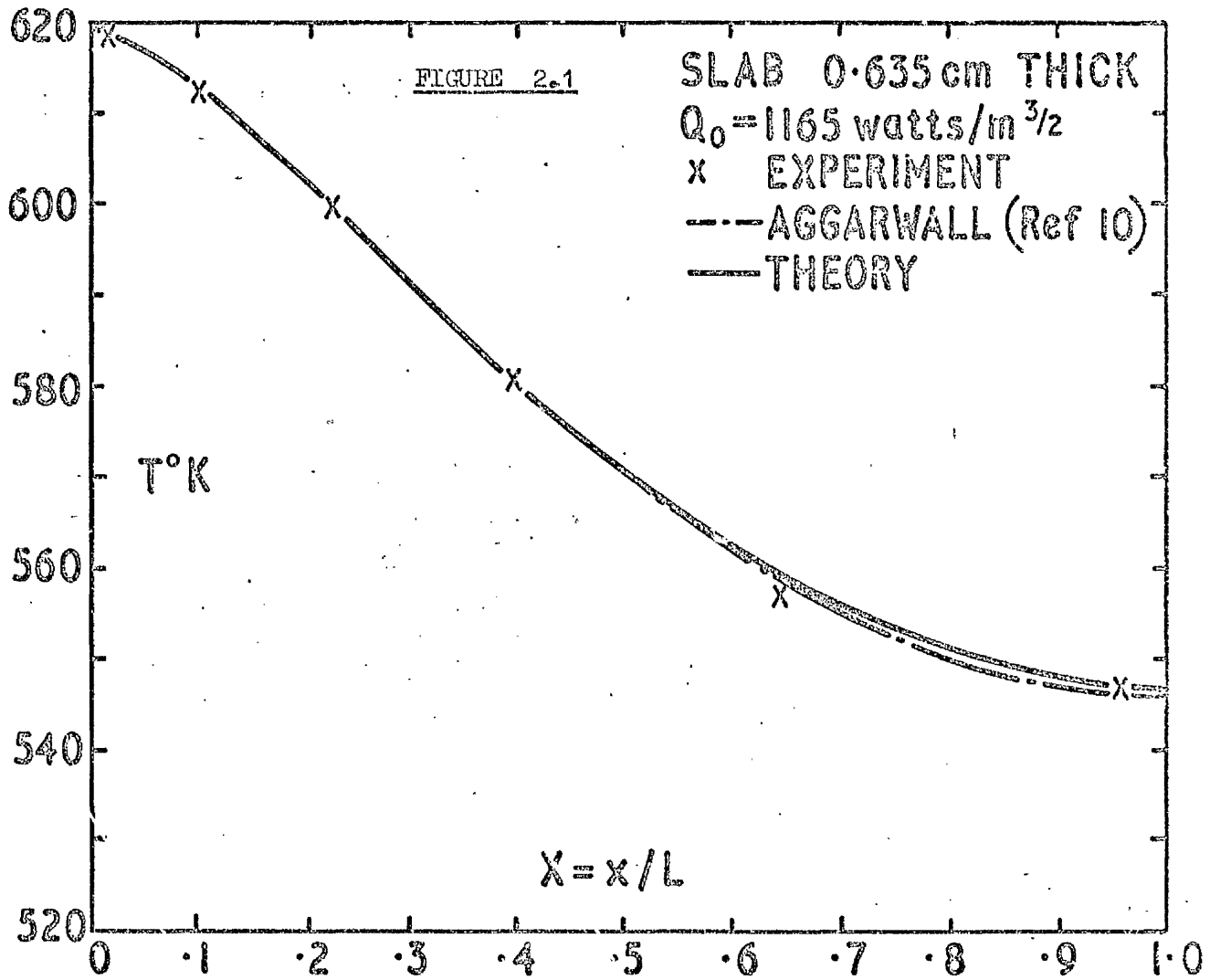
The present investigation is a continuation of work done in references 6 and 10. Further methods of reducing nose temperatures and of controlling the temperature distribution of the leading edge are examined. The basic theoretical and experimental procedures, laid down in references 6 and 10 are modified, where necessary, to cover the new topics of interest and to provide comparisons.

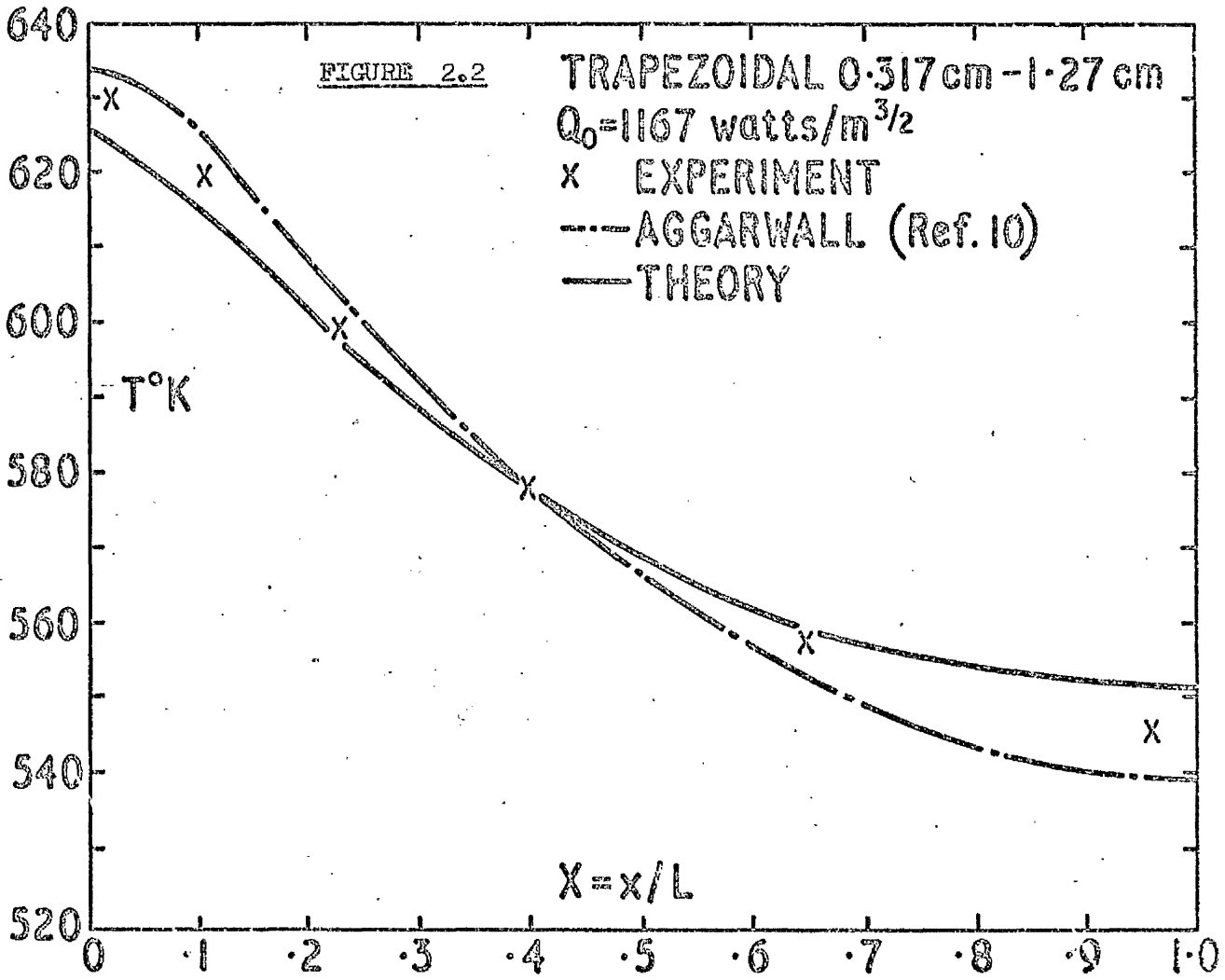
One of the conclusions arrived at in reference 10 was that if the thickness distribution of the leading edge was linear then the nose thickness, without taking into account the thickness variation, alone virtually determined the temperature distribution of the leading edge. During the present investigation this conclusion was found to be not entirely correct.

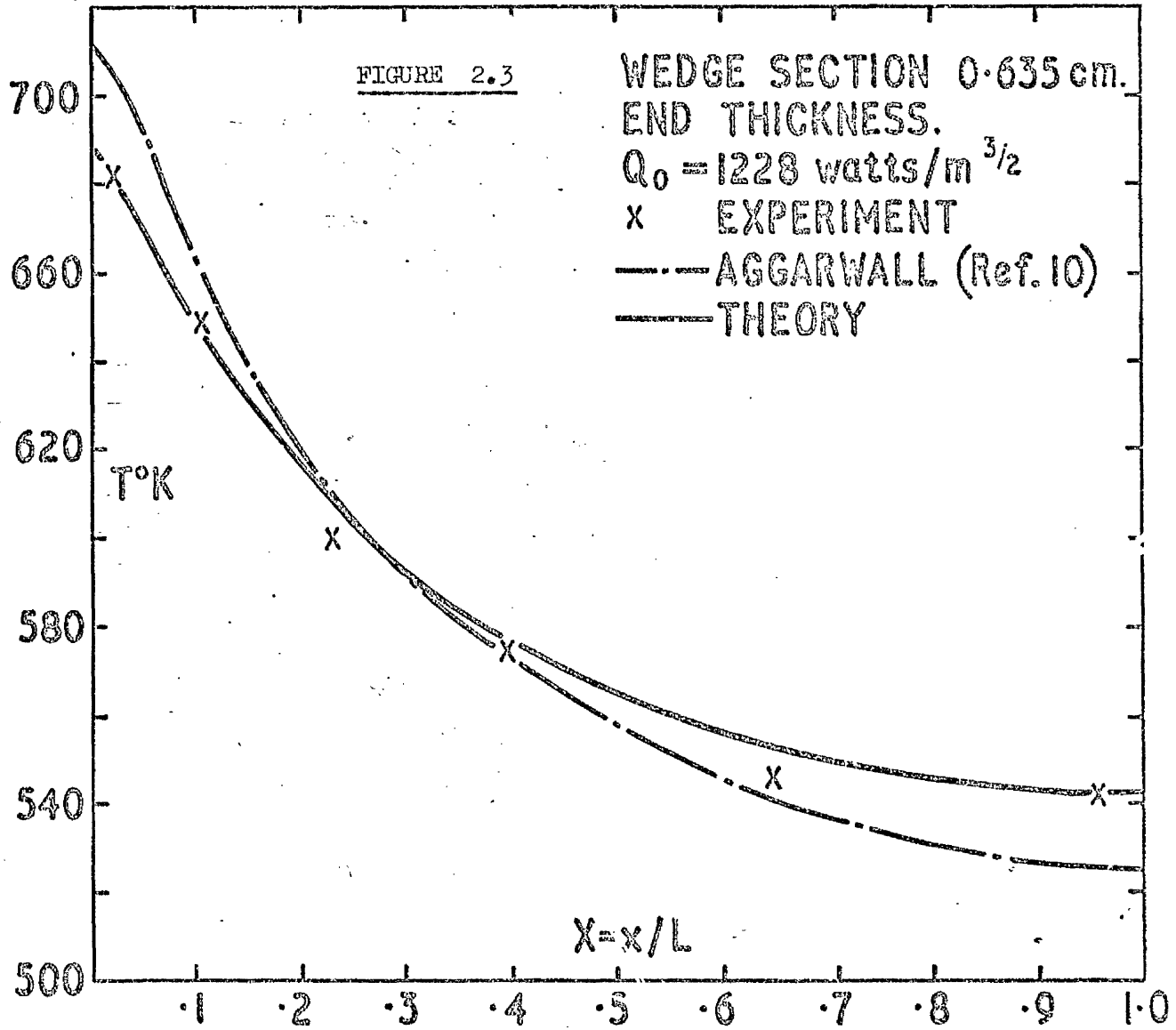
The effects of nose thickness on the temperature distribution can be taken as an indication of the volume of material present at the leading edge, but this assumption is not justifiable where the linear variation in thickness is large, such as a trapezoidal or wedge. The theoretical results for the nine models tested in Chapter IV of reference 10 were re-calculated allowing for the variation in thickness. Results for three of the models are shown in Figures 2. 1 - 3. The results showed no great differences between experimental results or the theoretical results calculated on the basis of nose thickness only, until models with large variations of thickness, such as wedges were encountered. Results for wedges showed greater agreement with experiment than the comparative theoretical results which did not allow for the variation in leading edge thickness. These results

therefore invalidate the conclusion arrived at in reference 10.

All theoretical results produced in this investigation are calculated on the basis that the thickness variation of the leading edge is taken into consideration. It is important that the effect on the nose temperature is due to the amount of the material concentrating at the nose and not due to the dimensional thickness of the nose alone.







CHAPTER III.Theoretical and Experimental Investigation of a Leading Edge
with a Highly Conducting Nose.3.1 Introduction

It has already been proved ^{6, 10} that the conducting power of the material situated at the leading edge is predominant in reducing the nose temperature. Further reduction of nose temperature could be achieved by increasing the conducting power of the material; this could be effected either by increasing the amount of material or by increasing the thermal conductivity of the material. This part of the investigation considers the latter method.

The thermal conducting ability of the leading edge is increased by bonding a nose strip of highly conducting material on to the basic structural material to form a composite leading edge. The main problem which arises is that a thermal resistance may be set up across the interface of the two structural materials and it is possible that the reduction gained in nose temperature will be offset by this thermal resistance.

A theoretical analysis of the composite leading edge was carried out using as a basis the conducting plate theory of reference 6. The formulation of the heat conduction equation for the composite leading edge had to be modified slightly compared to the general equation produced for the analysis of simple shapes without

any discontinuities. This was caused by the variation in material properties, such as emissivity, across the junction of the materials.

Experimentation for this investigation was carried out on models similar, in dimensions, to those in references 6 and 10, but fabricated with a nose of copper bonded on to a body of stainless steel. The experiments were conducted using the apparatus described in reference 10, and needed no modifications.

3.2 Theoretical Analysis of the Composite Leading Edge.

It is convenient, for simplicity of analysis, to envisage the leading edge region as 'a conducting plate.' The derivation of the heat conduction equation is based on the mathematical assumption that the thickness of the conducting plate is vanishingly small. If k is the thermal conductivity of the material, and t the thickness, then the product kt remains finite while the ratio t/k tends to zero. One of the important implications of this assumption is that within the body heat transfer normal to the surface can be ignored. Hence the dimensionality of the heat conduction equation is reduced by one.

3.2.1 Derivation of the Heat conduction Equation.

The modes of heat transfer, which are present when a hypersonic leading edge is subjected to aerodynamic heating are:-

- 1) Convective heat transfer from the boundary layer, $Q = f(x)$.
- 2) Heat radiated away from the surface - $\epsilon \sigma T^4$, where ϵ is the emissivity of the surface and σ the Stefan - Boltzmann constant.
- 3) Heat transferred inside the body by the conducting power of the material.

Since we are concerned with the temperature distribution and the temperature variation across the junction, we will take the heat conduction equation to be one - dimensional, x , origin at the nose, is measured in the chordwise direction. The heat conduction equation can then be defined as

$$\frac{d}{dx} \left(kt \frac{dT}{dx} \right) = \epsilon \sigma T^4 - Q(x) \quad 3.1$$

Thermal conduction plays a predominant role in moderating temperatures only over a particular length of the leading edge. Beyond this length, temperatures tend to the radiation equilibrium values. This length has been termed the 'conduction length'. Estimates of the size of the 'conduction length' were made in references 8 and 10. For practical considerations, the conduction length is liable to be substantially less than the length of model subjected to heating. Hence it is convenient to regard the conducting plate as being of bounded extent and length, L ; equation 3.1 will then be solved for the independent variable x/L .

It should be stated at this point that the product kt and the co-efficient ϵ can both be functions of temperature (T) and position (x).

Equation 3.1 yields two well-known solutions in the extreme. For $kt(x)$ tending to zero then

$$T = \left(\frac{Q(x)}{\epsilon \sigma} \right)^{\frac{1}{4}} \quad 3.2$$

i.e. the temperature is everywhere equal to the radiation equilibrium

value. The other extreme where $kt(x)$ tends to infinity yields the solution

$$T = \left(\frac{\int_0^L Q(x) dx}{\int_0^L \epsilon \sigma dx} \right)^{\frac{1}{4}} \quad 3.3$$

which is a constant temperature throughout, and corresponds to a plate of infinite conductivity.

Equation 3.1 was solved in references 6 and 10 subject to the boundary conditions that there is no longitudinal heat conduction at the nose ($x = 0$) and the tail ($x = L$). These can be written as

$$kt \frac{dT}{dx} = 0 \quad \text{at} \quad x = 0, L \quad 3.4$$

We have adopted the same convention in this investigation.

Throughout this analysis the convective heat input is assumed proportional to $(x + x_0)^{-\frac{1}{2}}$. Reference 10 provides detailed analysis of the reasoning behind the use of, and choice of value of, x_0 . Consequently we can now define the convective heat input as

$$Q = Q_0 / (x + x_0)^{\frac{1}{2}} \quad 3.5$$

where Q_0 is a constant.

We can now rewrite equation 3.1 more fully as

$$\frac{d}{dx} \left(kt \frac{dT}{dx} \right) = \epsilon \sigma T^4 - Q_0 / (x + x_0)^{\frac{1}{2}} \quad 3.6$$

Aggarwal¹⁰ formulated an equation, identical to 3.6 but in non-dimensional terms; in addition, Aggarwal solved the heat conduction equation by three different methods. The method, on which we base our solution of the conduction equation for the composite leading edge is a finite difference method in which the interval $x(0,L)$ divided into N equal intervals and the subsequent $N+1$ finite difference algebraic equations are solved iteratively by an explicit method, namely Gaussian elimination. Appendix A provides a thorough derivation of the algebraic finite difference equations for the heat conduction equation.

3.2.2. Modification of the heat conduction equation to deal with the variation of thermal properties of the composite materials.

Figure 3.2.2 is a representation of a conducting plate which corresponds to a leading edge with a highly conducting nose. The shape of the conducting plate as shown in figure 3.2.2 is of no importance

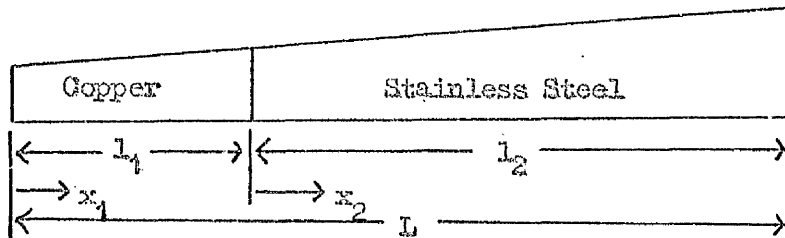


Figure 3.2.2

Consider the copper portion i.e. where $0 < x_1 < l_1$ and writing in the form of equation 3.1 we get

$$\frac{d}{dx_1} \left(kt \frac{dT}{dx_1} \right) = \epsilon_p T^4 - Q(x_1) \quad 3.7$$

where subscript 1 refers to copper and we define the convective

heat input as

$$Q(x_1) = Q_0 / (x_1 + x_0)^{\frac{1}{2}} \quad 3.8$$

For $0 < x_2 < l_2$, again applying equation 3.1 we get

$$\frac{d}{dx_2} \left(k_2 \frac{dT}{dx_2} \right) = \epsilon_2 \sigma T^4 - Q(x_2) \quad 3.9$$

where subscript 2 refers to stainless steel and again we define

$$Q(x_2) = Q_0 / (x_2 + l_1 + x_0)^{\frac{1}{2}} \quad 3.10$$

If the junction has negligible resistance to heat flow, then the temperatures on either side of the junction will be the same and the following equations will apply

$$\left(k_1 \frac{dT}{dx_1} \right)_{x_1 = l_1} = \left(k_2 \frac{dT}{dx_2} \right)_{x_2 = 0} \quad 3.11$$

which gives us

$$T_{x_1 = l_1} = T_{x_2 = 0} \quad 3.12$$

However if the junction has created a resistance to heat flow then the temperature will jump from material 1 to 2 across the joint so that at $x_1 = l_1$ we have $T = T_1$ and similarly at $x_2 = 0$ we have $T = T_2$. If we let R be the junction resistance, we then have

$$\left(k_1 \frac{dT}{dx_1} \right)_{x_1 = l_1} = \frac{1}{R} (T_1 - T_2) \quad 3.13$$

$$\left(k_2 \frac{dT}{dx_2} \right)_{x_2=0} = 0 = \frac{1}{R} (T_1 - T_2) \quad 3.14$$

It is obvious that if junction resistance, R , tends to zero then T_1 and T_2 will become identical. We can express R as

$$R = \frac{T_1 - T_2}{\left(k_1 \frac{dT}{dx_1} \right)_{x_1=l_1}} \quad 3.15$$

or

$$R = \frac{T_1 - T_2}{\left(k_2 \frac{dT}{dx_2} \right)_{x_2=0}} \quad 3.16$$

from which we obtain the expression

$$\left(\frac{dT}{dx_2} \right)_{x_2=0} = 0 = \frac{k_1}{k_2} \left(\frac{dT}{dx_1} \right)_{x_1=l_1} \quad 3.17$$

This would appear to be the same equation as 3.11, however the numerical values involved would be different since one equation assumes negligible resistance to heat flow across the junction, whilst the other does not.

The boundary conditions for the solution of the heat conduction equation, of a composite leading edge, now become:-

$$\text{at } x_1 = 0, \quad \frac{dT}{dx} = 0 \quad 3.18$$

$$\text{at } x_1 = l_1, \quad \frac{dT}{dx} = \left(\frac{dT_1}{dx_1} \right)_{x_1=l_1} \quad 3.19$$

$$\text{at } x_2 = 0, \quad \frac{dT}{dx} = \left(\frac{dT_2}{dx_2} \right)_{x_2=0} = 0 \quad 3.20$$

where from equation 3.13 we can write

$$T_2 = T_1 - R k_1 \left(\frac{dT_1}{dx_1} \right)_{x_1 = l_1} \quad 3.21$$

and finally at $x_2 = l_2$, $\frac{dT}{dx} = 0$ 3.22

The finite difference equations obtained in Appendix A for the general heat conduction equation (3.1) are solved, using Gaussian elimination, by a digital computer program. Appendix B shows how this program had to be altered to accommodate the composite leading edge.

3.2.3 Discussion of Theoretical Results.

Figures 3.2.3. 1-3 show theoretically calculated temperature distributions for three models which are representative of the type of models used to verify the general theory of conducting plates in references 6 and 10. The highly conducting nose is taken to be of copper and the main body of stainless steel. The reasons for this are outlined in section 3.3.2. The models were subjected to a convective heat input constant $Q_0 = 7500 \text{ W/M}^{3/2}$ and $x_0 = 0.004191 \text{ m}$. The temperature distributions are calculated on the basis of zero resistance to heat flow across the junction of the materials. Consequently the results can be viewed as being the best possible since a thermal resistance at the joint would produce a jump in temperature across it and a higher nose temperature.

The advantage of using a highly conducting nose are obvious from figures 3.2.3. 1-3. The benefits gained for a slab, Trapezoidal

FIGURE 3.2.3.1

SLAB 1.27cm THICK

Ⓐ STAINLESS STEEL

Ⓑ COPPER

Ⓒ COPPER - STAINLESS STEEL

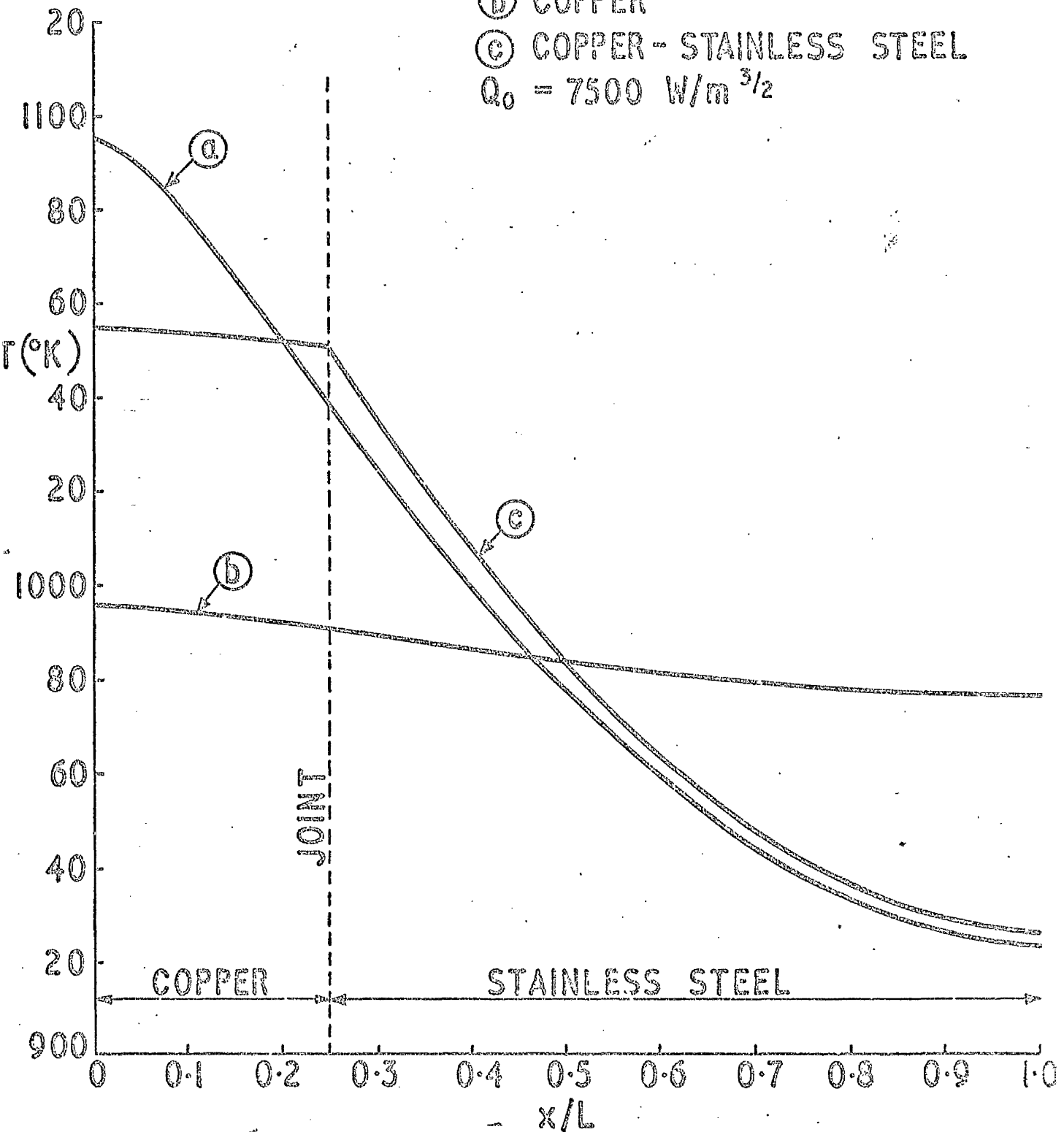
 $Q_0 = 7500 \text{ W/m}^{3/2}$ 

FIGURE 3.2.3.2

TRAPEZOIDAL 0.635 - 1.27 cm

- Ⓐ STAINLESS STEEL
 - Ⓑ COPPER
 - Ⓒ COPPER - STAINLESS STEEL
- $Q_0 = 7500 \text{ W/m}^{3/2}$

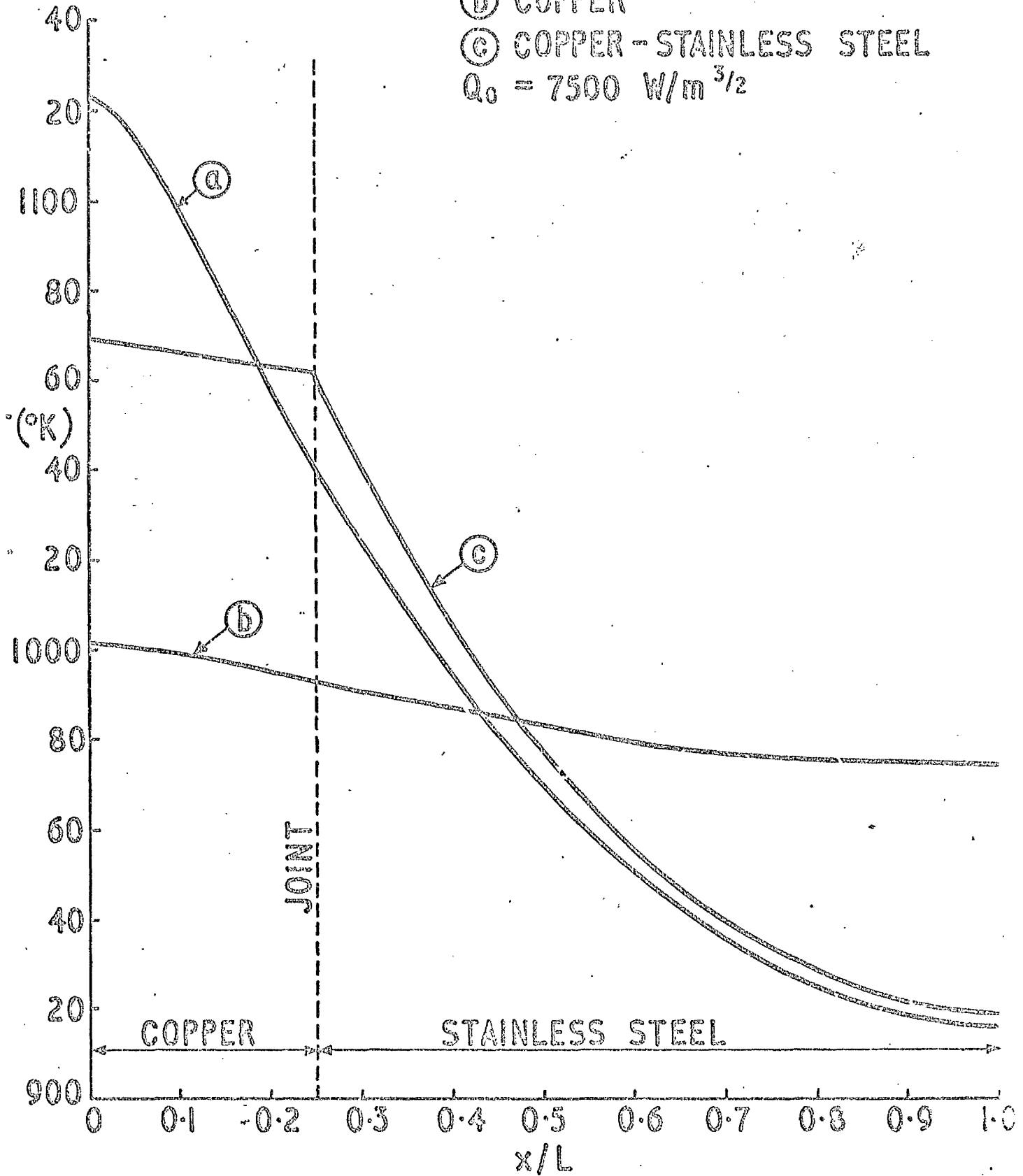


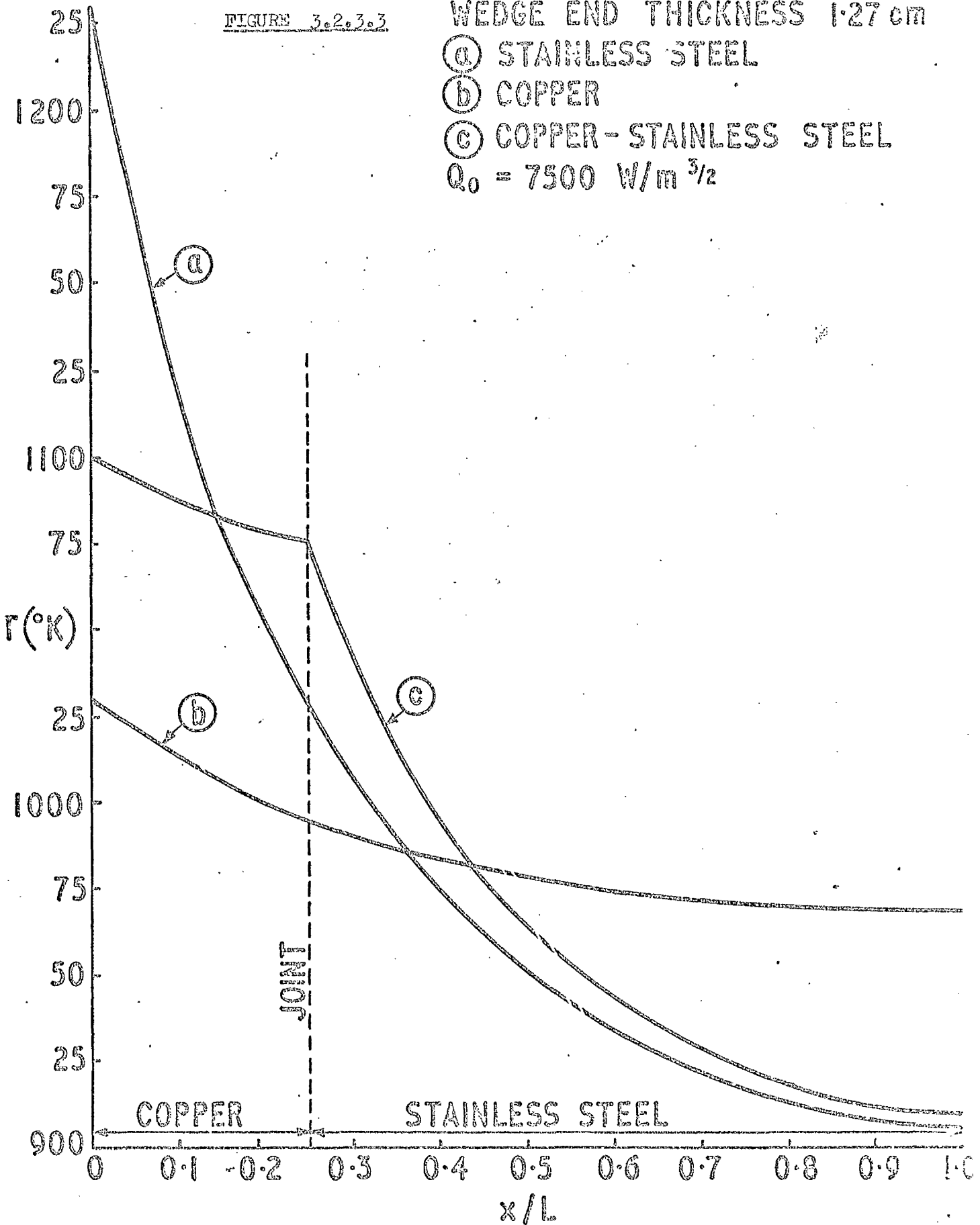
FIGURE 3.2.3.3

WEDGE END THICKNESS 1.27 cm

Ⓐ STAINLESS STEEL

Ⓑ COPPER

Ⓒ COPPER-STAINLESS STEEL

 $Q_0 = 7500 \text{ W/m}^{3/2}$ 

and wedge are respectively 3.6, 4.8 and 10.5% reduction in nose temperature compared to a leading edge of all stainless steel. The less material there is present at the nose then the more significant becomes the effect of the increased thermal conductivity of the leading edge. This suggests that a sharp leading edge, of a highly conducting material or composite material, could be constructed to produce the same nose temperature as a thicker leading edge of lower conductivity material. The figures for an all copper leading edge are produced for comparison with the all stainless steel and composite leading edges.

An investigation was carried out to find if the advantages gained by employing a highly conducting nose varied with heat input. The percentage reduction in nose temperature, based on an all stainless steel leading edge, was calculated for increasing values of Q_0 . The results for a typical example are shown in Figure 3.2.3.4. It should be noted that the vertical axis is sizeably enlarged and that over a range of Q_0 between 1,000 to 20,000 $\text{w/m}^{3/2}$ the percentage reduction in nose temperature varies between 4 and 5% but never exceeding 5%. If very fine limits of nose temperature were to be observed then a maximum reduction in nose temperature relative to convective heat input is available. Results for other shapes of models show very similar trends, the only varying value being the maximum reduction in nose temperature.

FIGURE 3.2.3.4.

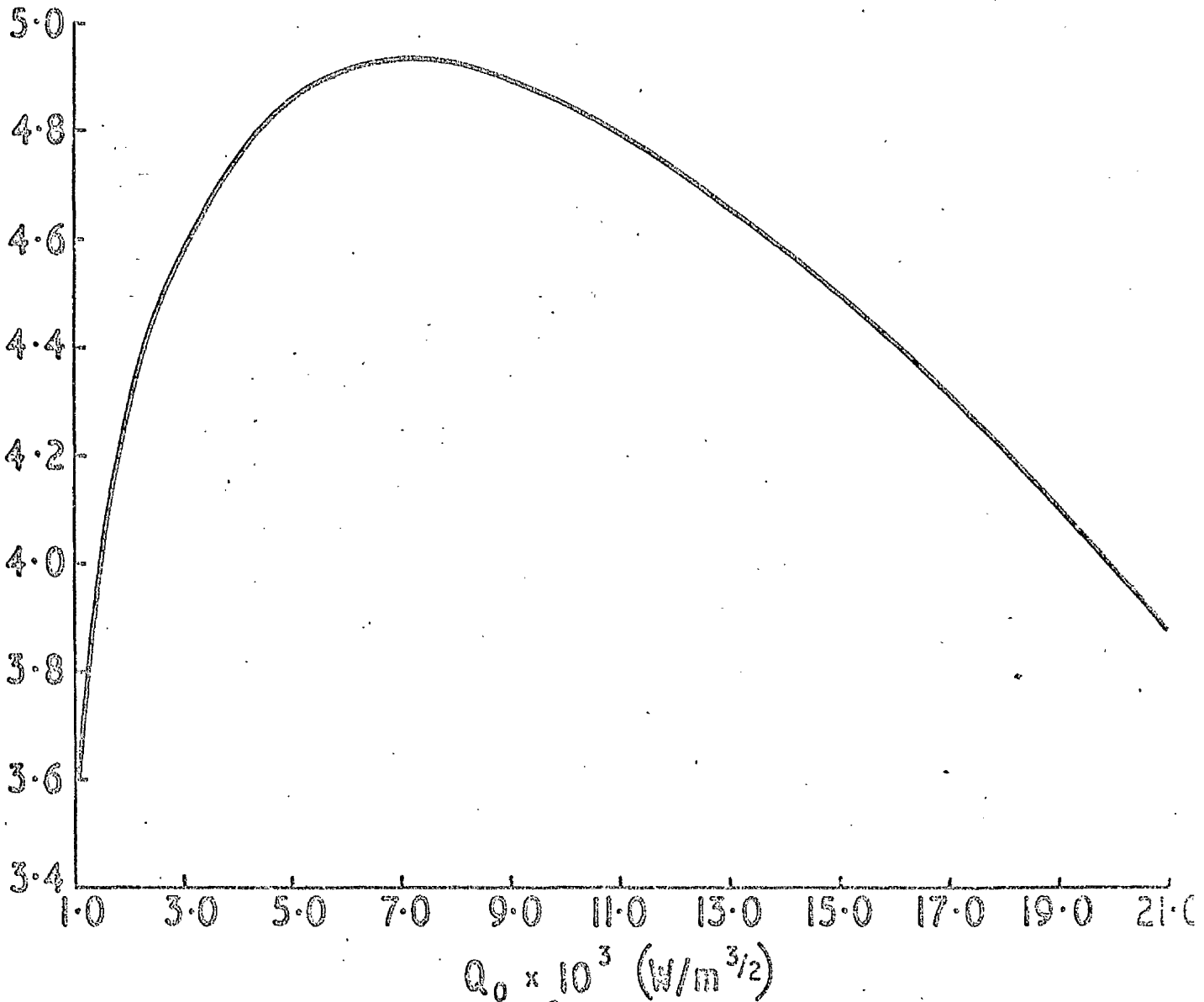
GRAPH OF % REDUCTION IN NOSE
TEMPERATURE

Vs

CONVECTIVE HEAT INPUT CONSTANT

 Q_0

FOR A TRAPEZOIDAL 0.635 - 1.27 cm

REDUCTION
IN NOSE
TEMPERATURE

3.3 Experimental Analysis of the Composite Leading Edge.

The purpose of the experimental analysis is to determine the junction thermal resistance which cannot be obtained analytically and to investigate the accuracy of the results predicted by the theoretical analysis. Models are manufactured to represent the leading edge and are subjected to simulated aerodynamic heating. The heat flux, which impinges on one surface of the model, corresponds approximately to $x^{-\frac{1}{2}}$ and is produced by the combination of an electric filament and specially designed reflector⁹. Aggarwal¹⁰ verified the general theory of conducting plates by testing several models which consisted of slabs, trapezoidals and wedges of varying dimensions. The apparatus used in reference 10 required no modification to test the models prepared for this investigation.

3.3.1 Simulation of Aerodynamic Heating.

The required heating distribution is provided by an electrically heated element as a source of infra - red radiation combined with a reflector. Sinha^{8,9} designed and constructed a reflector which produces a heat distribution approximately to $x^{-\frac{1}{2}}$ on a given irradiated plane. The reflector consists of seven curved surfaces which blend smoothly together to form a quasi-continuous profile.

The source of heat is a wire coiled round a ceramic (alumina) tube which is reinforced by the insertion of a tungsten rod through its centre to prevent sagging at high temperatures. Heating received by the model is due largely to the reflected

radiation and a very small percentage of direct radiation from the element.

The similarity laws derived in reference 9 permit us to carry out scaled experiments provided we select the parameters accordingly. The value of the heat input parameter, Q_0 , should be as high as possible so as not to restrict the use of materials to those with low co-efficients of thermal conductivity. In addition a higher value of Q_0 produces higher values of temperature everywhere within the model and reduces the effect of background temperature upon the temperature distribution. In the experimental investigation the value of Q_0 is directly proportional to the power dissipated in the heater filament. Aggarwal increased the power output capability of the filament compared to that of reference 8 and 9 by using tantalum instead of tungsten for the filament wire.

Aggarwal¹⁰ also thoroughly investigated the performance of the reflector using a radiometer¹¹ which was specially designed to measure the thermal radiation intensity over the model. The reflector was designed to simulate an $x^{-\frac{1}{2}}$ heat distribution over the model. Aggarwal found that very close to the leading edge the reflector could only produce finite and very limited rates of heat flux, but that over the range $x_0 < x < L$ the reflector reproduced the required distribution quite well, x_0 being very small compared to the length of the model. In practical terms it means that the nose of the model was placed at $x = x_0$ instead of $x = 0$.

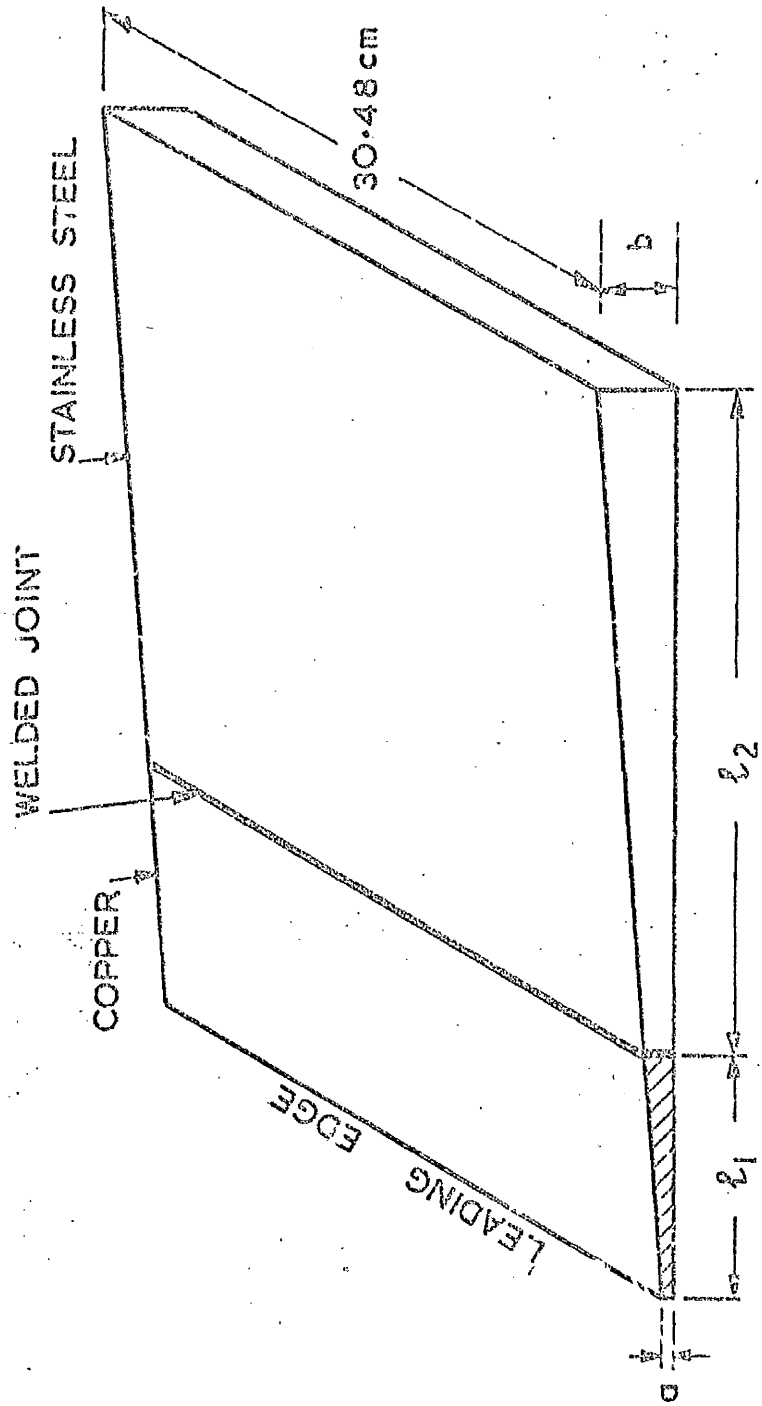
3.3.2 Test Models.

The size of the models are limited by the apparatus available; with the equipment available at present we can test models of planform area 0.3048×0.1524 m. The length, L , being fixed at 0.1524 m. The materials chosen for the composite leading edge were stainless steel for the main body and copper for the highly conducting nose. The particular type of stainless steel chosen was F.C.B. Staybrite also designated A.I.S.I. - 347. This type was chosen since it produced appreciable temperature difference from nose to tail during the experimental investigation of reference 10. Its co-efficient of thermal conductivity is given by the manufacturers¹² (Firth Vickers Stainless Steel Ltd.) as $k = 15.9(1 + 0.00039 \times T^{\circ}C) \text{ W/m}^{\circ}K$. Copper was chosen as the material for the conducting nose due to its availability and the fact that its value of thermal conductivity is approximately twenty five times that of F.C.B. Staybrite. It can therefore be safely assumed that the nose is 'highly conducting' as compared to the main body of the leading edge. The co-efficient of thermal conductivity for copper was taken as $k = 402.31(1 - 0.00016 \times T^{\circ}C) \text{ W/m}^{\circ}K$ and was obtained from Touloukian¹³.

Four models of trapezoidal section and linear variation of thickness were tested in all. The details regarding the dimensions of the four models are given in Table 3.3.2. Due to machining difficulties at the copper nose, L is not always exactly 0.1524 m. A typical test model is shown in figure 3.3.2.

Table 3.3.2 Test Models.

| Model No. | Material | Description |
|-----------|---|--|
| 1 | Copper Nose with Stainless Steel Body | Wedge a = 0.0508 cm b = 1.27 cm l ₁ = 3.023 cm l ₂ = 11.455 cm |
| 2 | " | Wedge a = 0.0254 cm b = 1.27 cm l ₁ = 3.947 cm l ₂ = 11.493 cm |
| 3 | " | Trapezoidal a = 0.3175 cm b = 1.27 cm l ₁ = 3.81 cm l ₂ = 11.43 cm |
| 4 | " | Trapezoidal a = 0.3175 cm b = 1.27 cm l ₁ = 3.782 cm l ₂ = 11.368 cm |



Leading edge model with a high thermal conducting nose.

FIGURE 3.3.2

3.3.3 Method of Bonding Copper Nose to Stainless Steel Body.

The bonding process is by brazing the two materials together as shown in Figure 3.3.2. The parts were roughly machined to size, with the contacting surfaces machined to a good mating fit. The surfaces were both 33 cms. long, one being approximately 0.4 cms. wide and the other 0.635 cms. The brazing process was carried out by R.A.E. Farnborough. Copper - silver eutectic was used as the filler metal, the application of which requires the plating of one junction surface with silver and the other with copper. The operation is carried out in a non - corrosive environment to avoid crevice corrosion at the junction. The copper surface of the nose piece was thus electroplated with 0.007 cms. thickness of silver and the stainless steel surface with a similar thickness of copper. The model was then supported in a simple metal jig, holding the brazing surfaces roughly in a horizontal plane by means of two vertical arms rising from a base plate and bolted to both pieces at the end, the copper piece being at the top. The assembly was then heated in a vacuum to a temperature of 800°C soaked for 20 minutes and then cooled quickly in an atmosphere of argon at low pressure.

The result of the brazing was proved very satisfactory; no failure was found in severe bending even after immersion in water for several days. Inspection also showed apparent fusion along the whole length of the joint.

3.3.4 Treatment of the Model Surface exposed to Radiation.

The top surface only of the model is exposed to thermal radiation. It should possess a high value of surface absorptivity in order to obtain as much as possible of the limited heating available. To minimise the effects of background radiation it is necessary to maximise the absolute measurements of temperature recorded on the model during the experiment. This would require that while we use a high value of surface absorptivity, the top surface should have a low emissivity. In practice however, it would be desirable for the surface of the wing to have a high value of surface emissivity to take full advantage of radiation cooling under equilibrium conditions.

A study was therefore undertaken to investigate the effects of various surface conditions on the variation of surface emissivity with temperature for the materials used in the experiment. An apparatus had previously been developed¹⁴, using an indirect heating method, to measure the total hemispherical emissivity of solid materials. Generally the total hemispherical emittance can be taken to be equal to the normal total emittance.

Based on the results of the investigation the surface of the model was shot - blasted with very fine grain shot and then evenly blackened by camphor soots. After this treatment the surface emissivity of the stainless steel was found to follow approximately the values given by $\epsilon = 0.675(1 - 0.000181 \times T^{\circ}\text{C})$ and that of copper as $\epsilon = 0.826(1 - 0.000365 \times T^{\circ}\text{C})$.

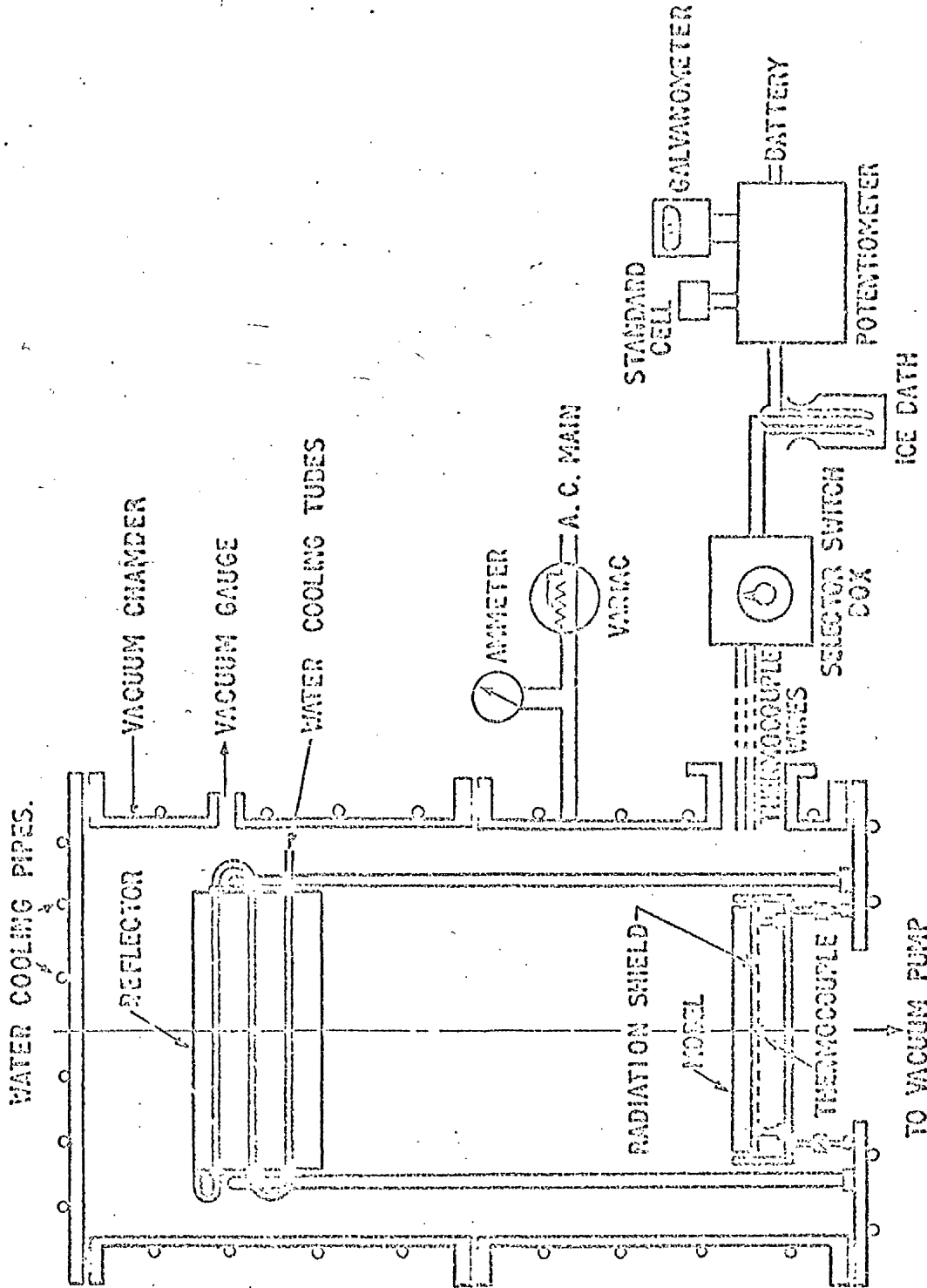
3.3.5 Apparatus and Experimental Procedure.

The models are subjected to heating inside a vacuum chamber. The purpose of carrying out the model tests in vacuum is to avoid convective heat transfer so that heat input to, and heat dissipation from, the model will be by thermal radiation alone. Heat transfer by natural convection¹⁵ becomes insignificant if the working pressure inside the vacuum chamber is maintained below 1 N/m^2 . The experiments are in fact conducted at pressures of the order of 2 mN/m^2 .

The inside walls of the vacuum chamber are painted black using an enamel paint which is claimed to have an absorptivity of 0.9. Any thermal radiation being reflected from the walls of the chamber is thus reduced to a minimum. Further, the vacuum chamber walls are water cooled so that the background radiation can be maintained at a low level.

Apart from the top surface of the model which is shot - blasted and blackened, the rest of the surfaces are highly polished using diamond powder. Additional shielding against radiation heat loss is provided by placing a highly reflecting surface parallel and close to the bottom polished face of the model. The experimental set-up is shown in Figure 3.3.5.1.

Heat loss by conduction from the model is reduced by resting it on four pointed ceramic pins, placed near the four corners. Heat transfer to the ceramic supports through four pin - points can thus be ignored. These pins are mounted on jacks which are used to



GENERAL LAYOUT OF APPARATUS

FIGURE 3.3.5.1

adjust the height of the model from a reference surface inside the vacuum chamber; with the help of this arrangement it is possible to set the top surface of the model precisely in the irradiated plane. In addition extra care is taken to ensure that the line of the leading edge is in the correct position.

Temperature measurements are taken at the middle section of the model, where one - dimensional conditions are expected to prevail, by means of thermocouples embedded into the material or where the thickness is insufficient by spot - welding the thermocouples on to the surface. The two methods give the same results. The thermocouples are made from 40 S W G (0.012 cm. diameter) Eureka - constantan wire; the wire diameter is small to reduce heat loss by conduction. In all eighteen thermocouples are placed in two rows (0.635 cm. apart) in the middle section of the model at nine prescribed locations. One row of thermocouples was placed near the top surface of the model and the other row near the bottom surface in order to detect any temperature variation across the model thickness. The thermocouples e.m.f. (which is a measure of the temperature) was recorded by means of a digital d.c. voltmeter.

The vacuum chamber is evacuated by means of a 6" diffusion pump backed by a single stage rotary pump. Once the working pressure of 2mN/m^2 (approximately 10^{-5} torr) is reached, the electrical power to the reflector filament is switched on and thereafter increased by definite increments. After each increment of power and as soon as steady state conditions are reached the temperature distribution in the model is recorded.

Table 3.3.5.1
Experimental Results.

| Model No. | Total power from heater (W) | Power received by model (W) | $Q_{o,3/2}$ (W/m ²) | Temperature Distribution °K | | | | | | | | |
|-----------|-----------------------------|-----------------------------|---------------------------------|-----------------------------|-------|-------|-------|-------|-------|-------|--------|--------|
| | | | | $\frac{x}{L} = .011$ | .094 | .22 | .24 | .26 | .28 | .45 | .70 | .98 |
| 1 | 1842 | 150.9 | 769.8 | 575.9 | 574.5 | 575.2 | 573.8 | 574.8 | - | 549.5 | 532.1 | 530.4 |
| | | | | 575.1 | 575.6 | 576.7 | 574.7 | 574.4 | - | - | - | - |
| 2 | 1849 | 198.6 | 983.1 | 610.3 | 607.4 | 608.9 | 608.8 | 605.2 | 601.1 | 575.6 | 558.3 | 550.9 |
| | | | | - | 604.0 | 609.0 | 608.7 | 604.7 | 600.4 | 575.7 | 551.6 | 550.9 |
| 3 | 1881 | 178.67 | 890.88 | 592.4 | 591.6 | - | 588.9 | 584.8 | - | 566.0 | 545.5 | 540.74 |
| | | | | 592.32 | 591.9 | 590.4 | 590.0 | 588.3 | - | 570.4 | 550.36 | 540.71 |
| 4 | 1844 | 166.4 | 832.1 | 580.2 | 579.5 | 577.5 | 578.0 | 576.3 | 574.0 | 554.2 | 539.2 | 533.1 |
| | | | | 576.7 | 579.3 | 578.3 | 577.6 | 575.8 | 572.9 | - | 533.5 | 528.5 |

Note: For each model the upper row temperatures were taken near the top surface while the lower row temperatures near the bottom surface.

Table 3.3.5.1 gives the results of the four models that have been tested. Only the comparisons between the temperature distributions corresponding to the maximum power and the theoretical values are presented later in the discussion. Note that less than 10% of heat dissipated in the filament is in fact absorbed by the model.

3.3.6 Experimental Errors.

Whereas every precaution is taken to eliminate any experimental errors, there are certain errors which are unavoidable. These errors are listed briefly

- 1) Although convective heat transfer can be ignored at pressures below 2mN/m^2 , heat transfer by free - molecular conduction may exist, however, under the prevalent conditions it can be taken as negligible.
- 2) A very small amount of heat is lost through the thermocouple wires, but this is unavoidable and negligible compared with the longitudinal conduction of heat.
- 3) Except the top surface, all the other surfaces are highly polished and shielded against heat loss. However some heat loss from the sides is inevitable.
- 4) The Eureka - constantan thermocouples used to measure temperature have been calibrated at the National Physical Laboratory to within $\pm 0.2^\circ\text{C}$.
- 5) A small amount of heat is reflected from the vacuum chamber walls on to the model.
- 6) Back - ground radiation from the vacuum chamber walls which are

maintained at the cooling temperature.

- 7) The reflecting surface of the reflector is becoming less perfect after several years use and consequently the heating simulation is less efficient.

3.3.7 Discussion and Comparison of Theory with Experiment.

Figures 3.3.7 1-4 show experimental results for the four models tested and comparisons with the theoretical results for the same heat input and model dimensions. The convective heat input constant, Q_0 , is calculated from the experimental results, using a numerical integration method and the equation

$$\sigma \int_0^L \epsilon T^4 dx = \int_0^L Q_0 / (x + x_0)^{\frac{1}{2}} dx \quad 3.3.7$$

This equation represents the conditions under which the models are tested i.e. the total input of heat to the model must equal the total amount of heat radiated away from the model.

The agreement between theory and experiment is good. The difference between the theoretical and experimental results for the composite leading edge does not exceed 1.5% anywhere over the model. Since the theoretical results are based on zero resistance to heat flow across the junction and the experimental results show good agreement with the theoretical, then the resistance to heat flow at the model junction can be taken as negligible.

Several errors which could have an effect on the theoretical results have arisen. A curve has to be drawn from the experimental

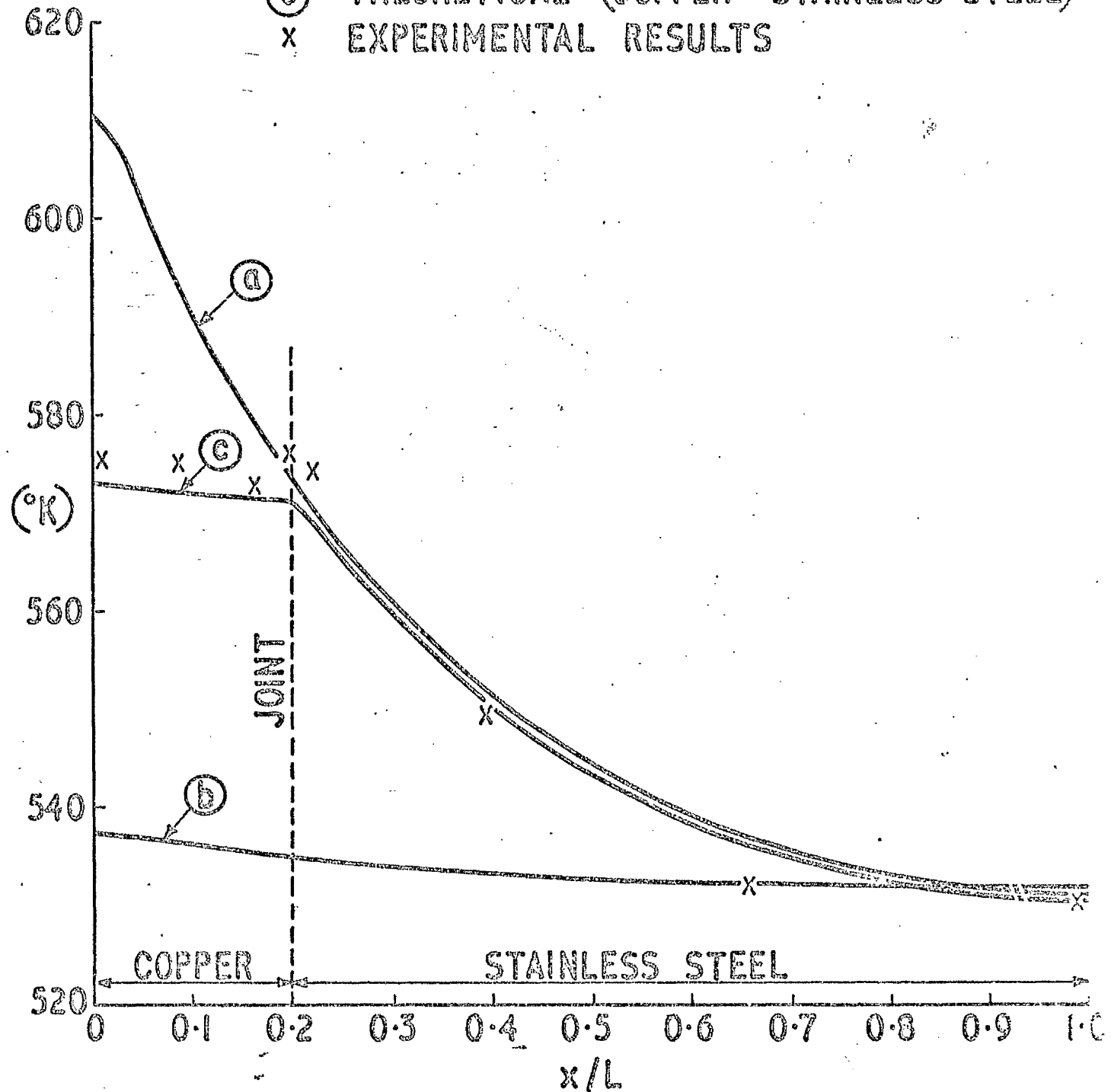
FIGURE 3.3.7.1

COMPOSITE MODEL I

WEDGE SECTION END THICKNESS 1.27 cm

$$Q_0 = 769.8 \text{ W/m}^{3/2}$$

- (a) THEORETICAL (STAINLESS STEEL)
- (b) THEORETICAL (COPPER)
- (c) THEORETICAL (COPPER - STAINLESS STEEL)
- x EXPERIMENTAL RESULTS



WEDGE SECTION END THICKNESS 1.27 cm

$Q_0 = 983.1 \text{ W/m}^{3/2}$

- (a) THEORETICAL (STAINLESS STEEL)
- (b) THEORETICAL (COPPER)
- (c) THEORETICAL (COPPER - STAINLESS STEEL)
- x EXPERIMENTAL RESULTS

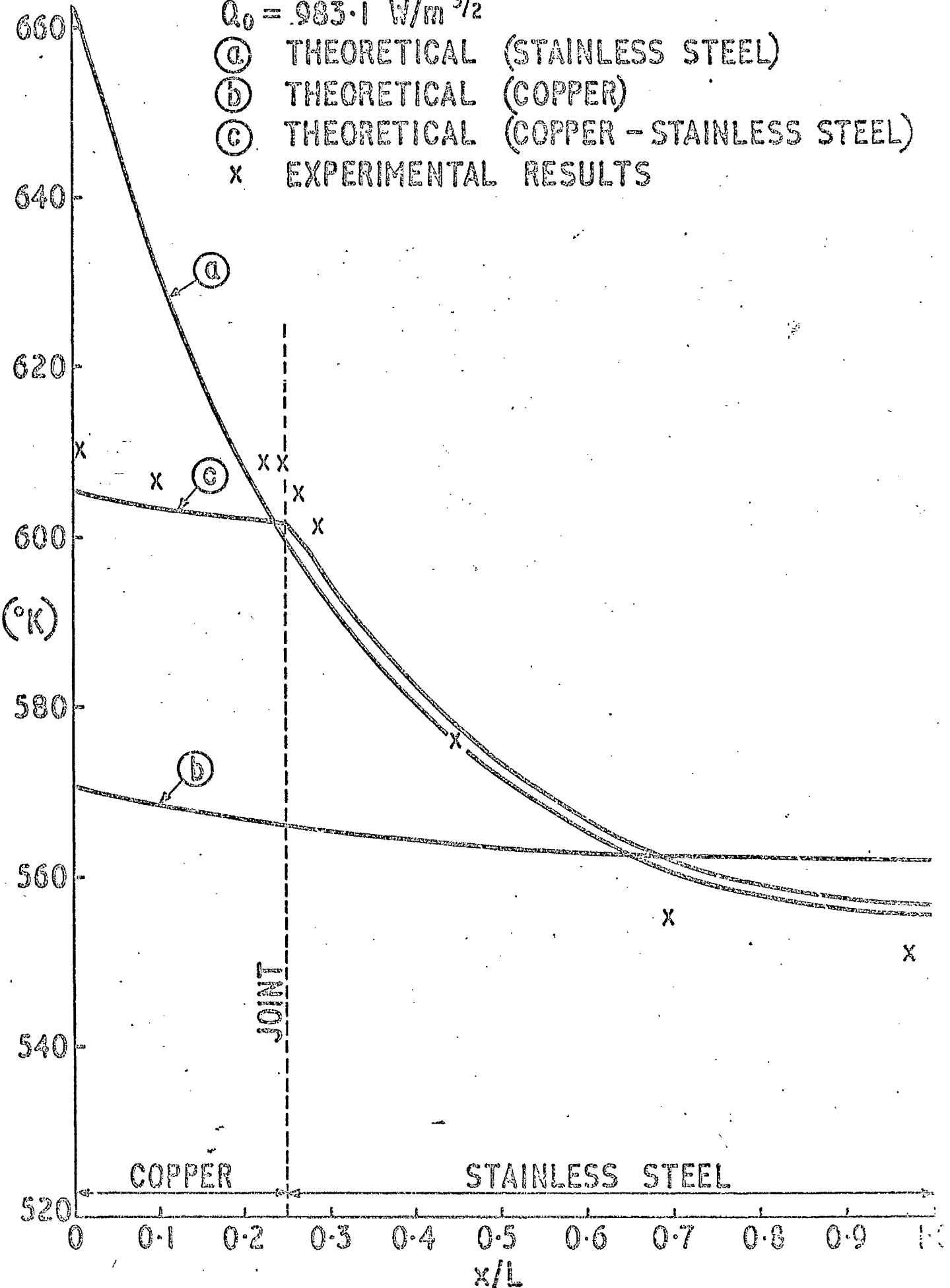


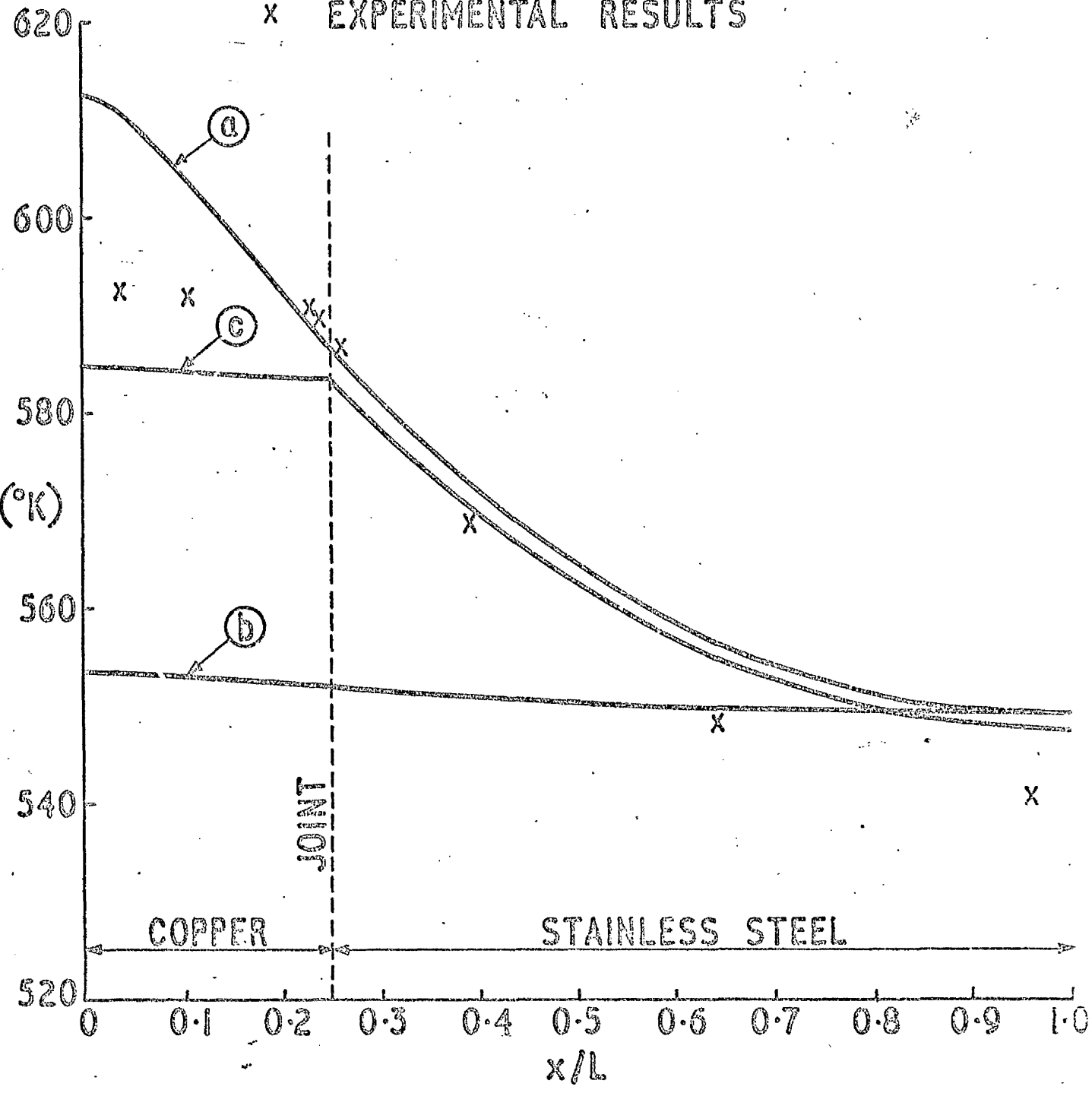
FIGURE 3.3.7.3

COMPOSITE MODEL 3

TRAPEZOIDAL SECTION 0.3175 - 1.27 cm

$Q_0 = 890.9 \text{ W/m}^{3/2}$

- Ⓐ THEORETICAL (STAINLESS STEEL)
- Ⓑ THEORETICAL (COPPER)
- Ⓒ THEORETICAL (COPPER - STAINLESS STEEL)
- x EXPERIMENTAL RESULTS



results to provide enough points to make the numerical integration, from which we get Q_0 , sufficiently accurate. If the curve deviates from the experimental results then the value of Q_0 will be affected, since we have to calculate the amount of heat radiated from the surface of the model, which is proportional to T^4 . Thus if there is a 1% change in T then there will be a 4% change in the amount of heat radiated from the model and hence a similar change in Q_0 . It is very difficult to measure accurately the nose thickness of trapezoidal or wedge models due to the rounding - off of the nose during machining. The value of thermal conductivity for copper was taken from Touloukian ¹³; this reference assumed the copper to be of high purity. The copper used to construct the models was not as pure as that of reference 13 and consequently the value of thermal conductivity may deviate from the quoted values.

In all the models, two rows of thermocouples were embedded at two different depths to detect any temperature gradients across the thickness of the material. Consistent with the basic assumption, no significant temperature variations across the thickness were measured.

CHAPTER IV.Investigation of the effect of the shape of the Leading Edge.4.1 Introduction.

Recent investigations in leading edge heating problems have been concerned only with theoretical and experimental studies of relatively simple leading edge shapes. The object of the investigation is to find the material distribution for a leading edge such that it has a minimum nose temperature for the material available and a linear temperature distribution over its length.

A theoretical analysis was carried out to calculate the thickness distribution of a leading edge which would fit the above requirements. The analysis is considerably simplified, by choosing a linear temperature distribution, since the heat conduction becomes directly integrable. A linear temperature distribution also produces a stress-free leading edge. It was found that the thickness distribution, to fulfill the required conditions, was directly related to the convective heat input constant Q_0 . This relationship presented problems in the experimental investigation.

The amount of heat input available to the experimental models, from our apparatus, is not very high and consequently, according to the similarity laws⁶, the models must be thin. Great difficulties had to be overcome during manufacture of the experimental models in order to produce the required thickness variation. The experimental

model was tested using the apparatus described in Chapter III

4.2 Theoretical Analysis of the Leading Edge.

The heat conduction equation as derived in chapter III for a leading edge subjected to aerodynamic heating can be written as

$$\frac{d}{dx} \left(kt \frac{dT}{dx} \right) = \epsilon \sigma T^4 - Q(x) \quad 4.1$$

The temperature distribution for the leading edge is taken as linear and can be written as

$$T = T_0 - \alpha x \quad 4.2$$

where T_0 and α are constants, equal to nose temperature and variation of temperature with length respectively and x is measured in the chordwise direction from the nose.

If we integrate equation 4.1 whilst substituting with equation 4.2 we get

$$\alpha kt = H(x) + \frac{\epsilon \sigma}{5 \alpha} (T^5 - T_0^5) \quad 4.3$$

where $H(x) = \int_0^x Q(x) \cdot dx$ and where we have used the fact that $t = 0$ at $x = 0$. If we also assume that $kt = 0$ at $x = L$, where L is the length of the model then

$$H(L) = \frac{\epsilon \sigma}{5 \alpha} [T_0^5 - (T_0 - \alpha L)^5] \quad 4.4$$

and further if we suppose that the cross-sectional area of the thickness distribution is A then integrating equation 4.3 again we get

$$\alpha kA = \int_0^L H(x) \cdot dx + \frac{\epsilon \sigma}{30 \alpha^2} [T_0^6 - (T_0 - \alpha L)^6] - \frac{\epsilon \sigma}{5 \alpha} T_0^5 L \quad 4.5$$

Thus with known $Q(x)$, L , ϵ , σ and kA equations 4.4 and 4.5 determine T_0 and α and 4.3 provides the associated thickness distribution.

However there must be some relationship between T_0 and L (assuming that $Q(x)$, ϵ , σ and kA remain fixed) which renders T_0 a minimum. If we regard T_0 , α and L as independent variables in equations 4.4 and 4.5 then from 4.5, and employing calculus of variations,¹⁷ we get

$$\left\{ kA + \frac{\epsilon \sigma}{15 \alpha^3} (T_0^6 + T_L^6) - \frac{\epsilon \sigma}{5 \alpha^2} (T_0^5 + T_L^5) L \right\} \delta \alpha \\ = \left\{ H(L) - \frac{\epsilon \sigma}{5 \alpha} (T_0^5 - T_L^5) \right\} \delta L + \left\{ \frac{\epsilon \sigma}{5 \alpha^2} (T_0^5 - T_L^5) - \frac{\epsilon \sigma T_0^4 L}{\alpha} \right\} \delta T_0$$

where $T_L = T_0 - \alpha L$ and so from equation 4.4 the term involving δL is zero and hence if T_0 has a stationary value (i.e. $\delta T_0 = 0$) then α also has a stationary value. Applying the same principle to equation 4.4 we get

$$\alpha (Q(L) - \epsilon \sigma T_L^4) \delta L = \epsilon \sigma (T_0^4 - T_L^4) \delta T_0 + (\epsilon \sigma T_L^4 L - H(L)) \delta \alpha$$

and consequently δT_0 will be zero when

$$\epsilon \sigma T_L^4 = Q(L) \quad 4.6$$

which from 4.1 implies that $\frac{dt}{dx} = 0$ at $x = L$, i.e. the trailing edge of the thickness distribution is cusped. Equations 4.4, 5 and 6 now determine T_0 , α and L for fixed $Q(x)$, ε , σ and kA such that T_0 is a minimum.

To obtain a thickness distribution, it is easier to assume a value of L and then calculate the thickness distribution for which this selected L is optimum. Thus with known L , equation 4.6 gives us T_L directly and further, noting that $T_0 = T_L + \alpha L$, we can rewrite 4.4. as

$$\frac{1}{2} \left\{ \left[\frac{H(L)}{L Q(L)} \right] - 1 \right\} = \left(\frac{\alpha L}{T_L} \right) + \left(\frac{\alpha L}{T_L} \right)^2 + \frac{1}{2} \left(\frac{\alpha L}{T_L} \right)^3 + \frac{1}{10} \left(\frac{\alpha L}{T_L} \right)^4 \quad 4.7$$

The left - hand side is easily determined and has been plotted against $(\alpha L/T_L)$ in Figure 4.2.1. From this graph we get the value of $(\alpha L/T_L)$ and hence α and so of T_0 . Equation 4.3 then allows kt to be determined and with it the optimised thickness distribution. This method of producing the thickness distribution is very convenient since the value of L will be fixed by our experimental conditions.

Throughout this part of the investigation the convective heat input function, $Q(x)$ can be taken as

$$Q(x) = Q_0 / (x + x_0)^{\frac{1}{2}} \quad 4.8$$

where Q_0 and x_0 have their usual meaning. We take $H(x) = \int_0^x Q(x) dx$

and this provides us with

$$H(L) = 2 Q_0 \left\{ (L + x_0)^{\frac{1}{2}} - x_0^{\frac{1}{2}} \right\} \quad 4.9$$

which in turn gives us

$$\int_0^L H(x) dx = 2 Q_0 \left\{ \frac{2}{3} (L + x_0)^{\frac{3}{2}} - L x_0^{\frac{1}{2}} - \frac{2}{3} x_0^{\frac{3}{2}} \right\} \quad 4.10$$

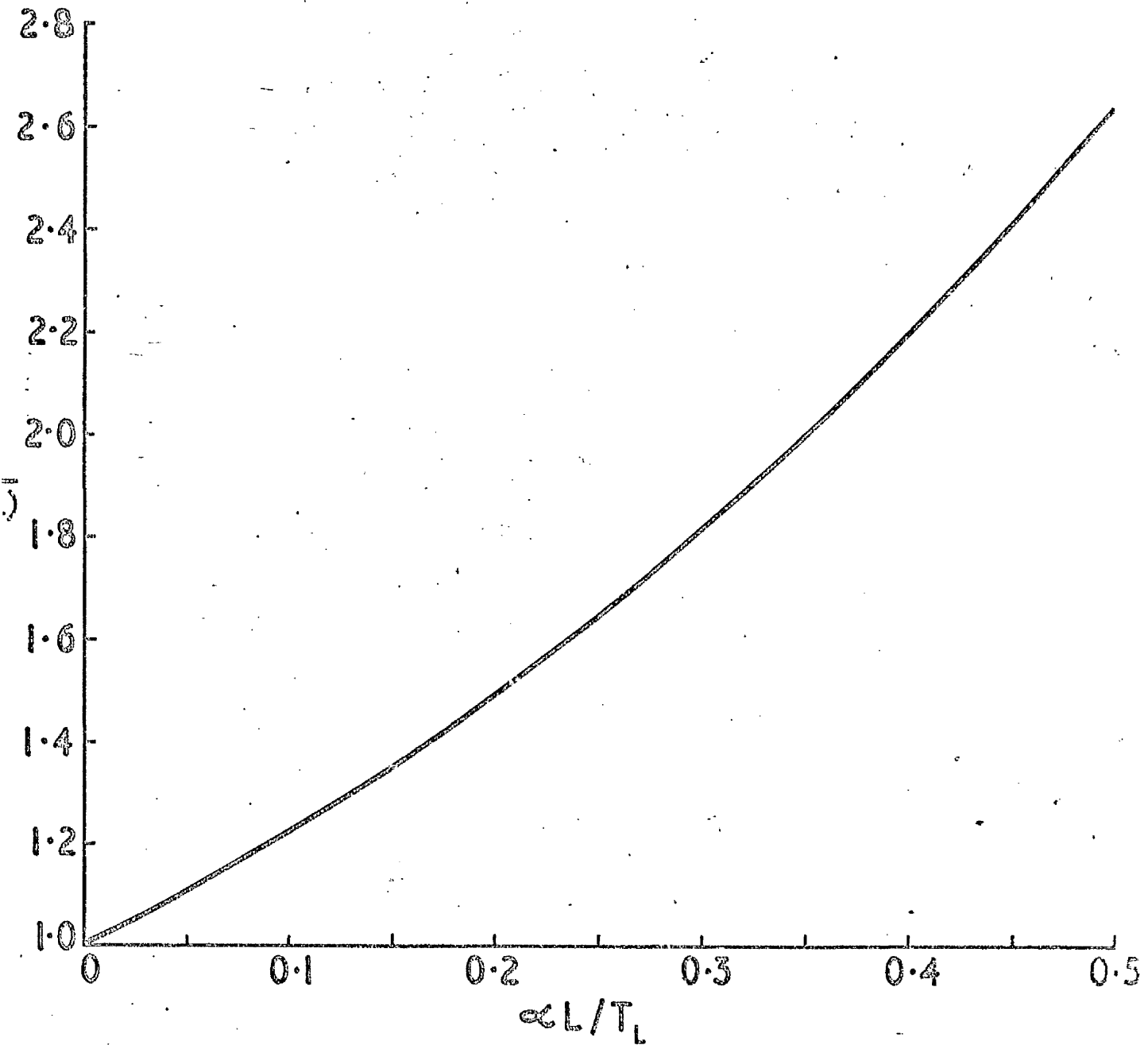
from these results it can be seen that $H(L) / IQ(L)$ is independent of Q_0 , which means that Figure 4.2.1 provides a relationship between $\alpha L / T_L$ and $H(L) / IQ(L)$ for any value of Q_0 provided L is fixed.

4.3. Theoretical Results and Discussion.

The most convenient method of calculating required optimum shapes and nose temperatures is to assume a value of length and calculate the cross-sectional area of leading edge for which this selected value of L is an optimum. This method of calculation is particularly suited to our requirements since the value of L is limited by the experimental conditions available.

To provide comparisons with other shapes of leading edge, cross-sectional areas of leading edges which would have minimum nose temperatures were calculated for varying values of Q_0 ; temperature distributions were then obtained for slabs, trapezoidals and wedges of exactly the same area, as the optimised shape leading edge, subjected to the same heat input. The results are shown in

FIGURE 4.2.1

PLOT OF $H(L)/LQ(L)$ Vs $\alpha L/T_L$ 

Figures 4.3.1-3. Reasons for choosing $Q_0 = 1250 \text{ W/m}^{3/2}$ will be given later, the other two sets of results are merely examples which are indicative of the values obtained over a wide range of values of Q_0 . The value of x_0 is fixed, as before, at 0.004191 m.

The actual values of nose temperature do not really concern us, the important factor is the benefit which is gained by using an optimised shape as compared to other shapes. The variations of nose temperature between the slab and trapezoidal shapes compared to the optimised shape are reductions of 2% and 3% respectively. The difference in nose temperature between the wedge and optimised shape is considerably larger and increases with increasing value of Q_0 . At $Q_0 = 1250 \text{ W/m}^{3/2}$ the difference is 7.5%, rising to 9.25% at $Q_0 = 5000 \text{ W/m}^{3/2}$ and 10% at $Q_0 = 10,000 \text{ W/m}^{3/2}$. These results are of considerable significance since of the three shapes compared with the optimised shape the wedge would be taken as the nearest approximation to an actual aircraft wing.

The procedure can be reversed by fixing A , the cross-sectional area, and allowing L to be variable. This method requires an iterative form of solution since Figure 4.2.1 holds true only when the value L is constant. To overcome this a simple computer program was written to solve iteratively for L . As an example we set $Q_0 = 1250 \text{ W/m}^{3/2}$ and $A = 5 \text{ cm}^2$; for this cross-sectional area to have a minimum value of nose temperature L must equal 0.1791 m. and the value of nose temperature is 644.3°K . Comparing these results with the case where L is fixed, A is variable and the heat input

FIGURE 4.3.1

$$Q_0 = 1250 \text{ W/m}^{3/2} \quad A = 3.1627 \text{ cm}^2$$

$$\epsilon = 0.8 \quad k = 17.78 \text{ W/m}^\circ\text{K}$$

$$L = 0.1524 \text{ cm}$$

- Ⓐ WEDGE 0.389 cm END THICKNESS
- Ⓑ TRAPEZOIDAL 0.138 - 0.277 cm
- Ⓒ SLAB 0.2075 cm THICK
- Ⓓ OPTIMISED NOSE TEMPERATURE

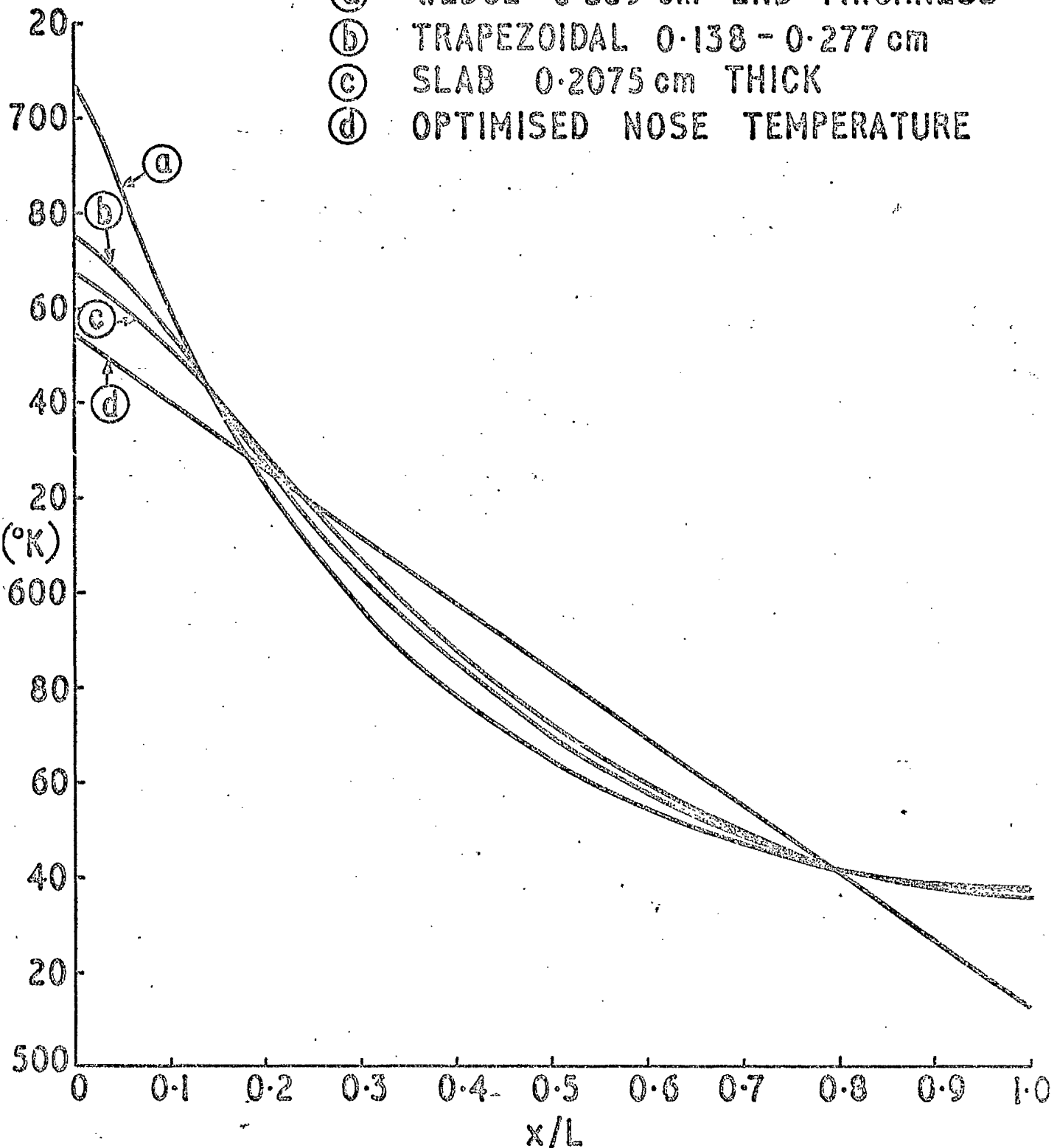


FIGURE 4.3.2

$Q_0 = 5000 \text{ W/m}^{3/2}$

$A = 8.9455 \text{ cm}^2$

$\epsilon = 0.8$

$k = 17.78 \text{ W/m}^\circ\text{K}$

$L = 0.1524 \text{ cm}$

- Ⓐ WEDGE 1.1485 cm END THICKNESS
- Ⓑ TRAPEZOIDAL 0.392 - 0.783 cm
- Ⓒ SLAB 0.586 cm THICK
- Ⓓ OPTIMISED NOSE TEMPERATURE

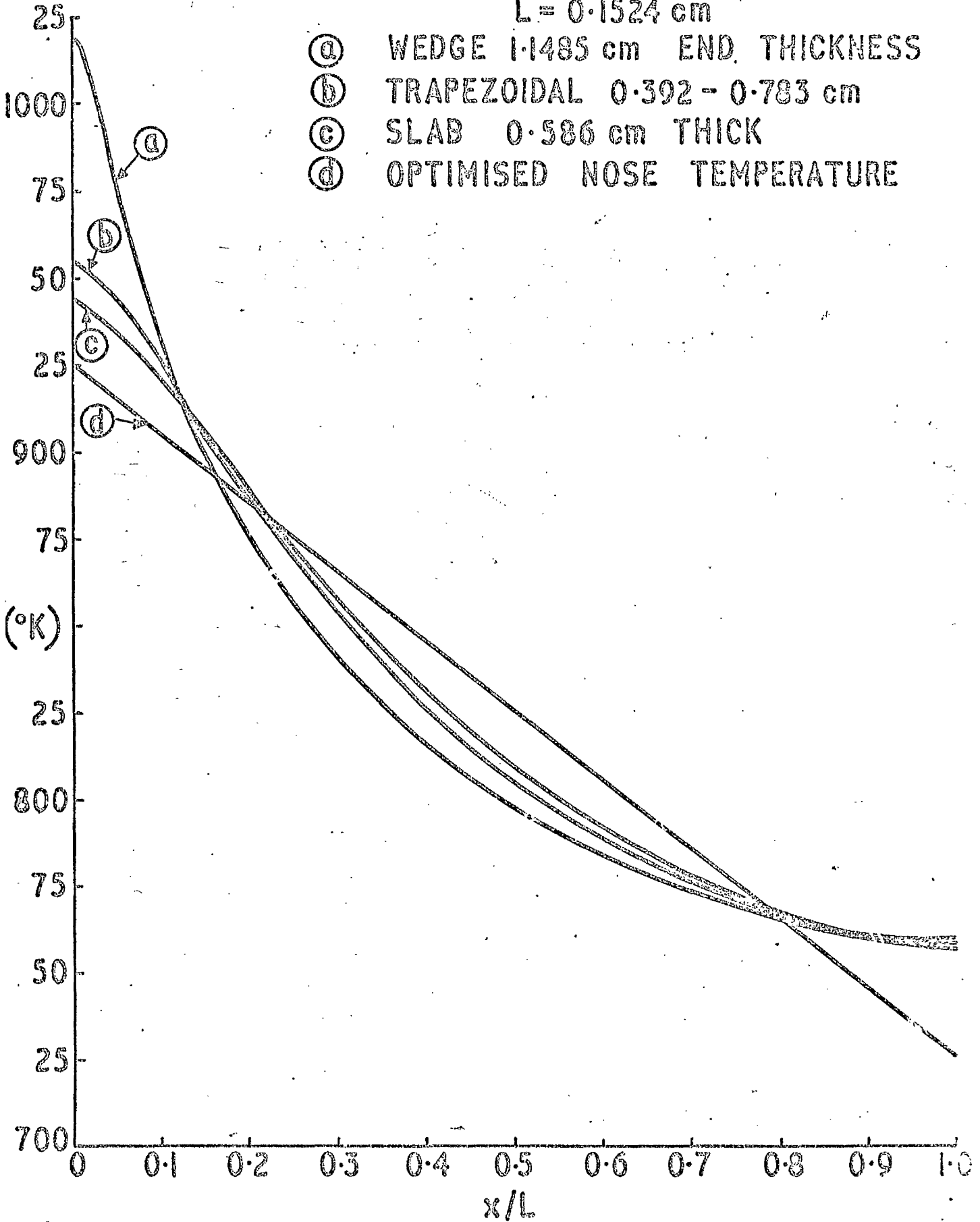


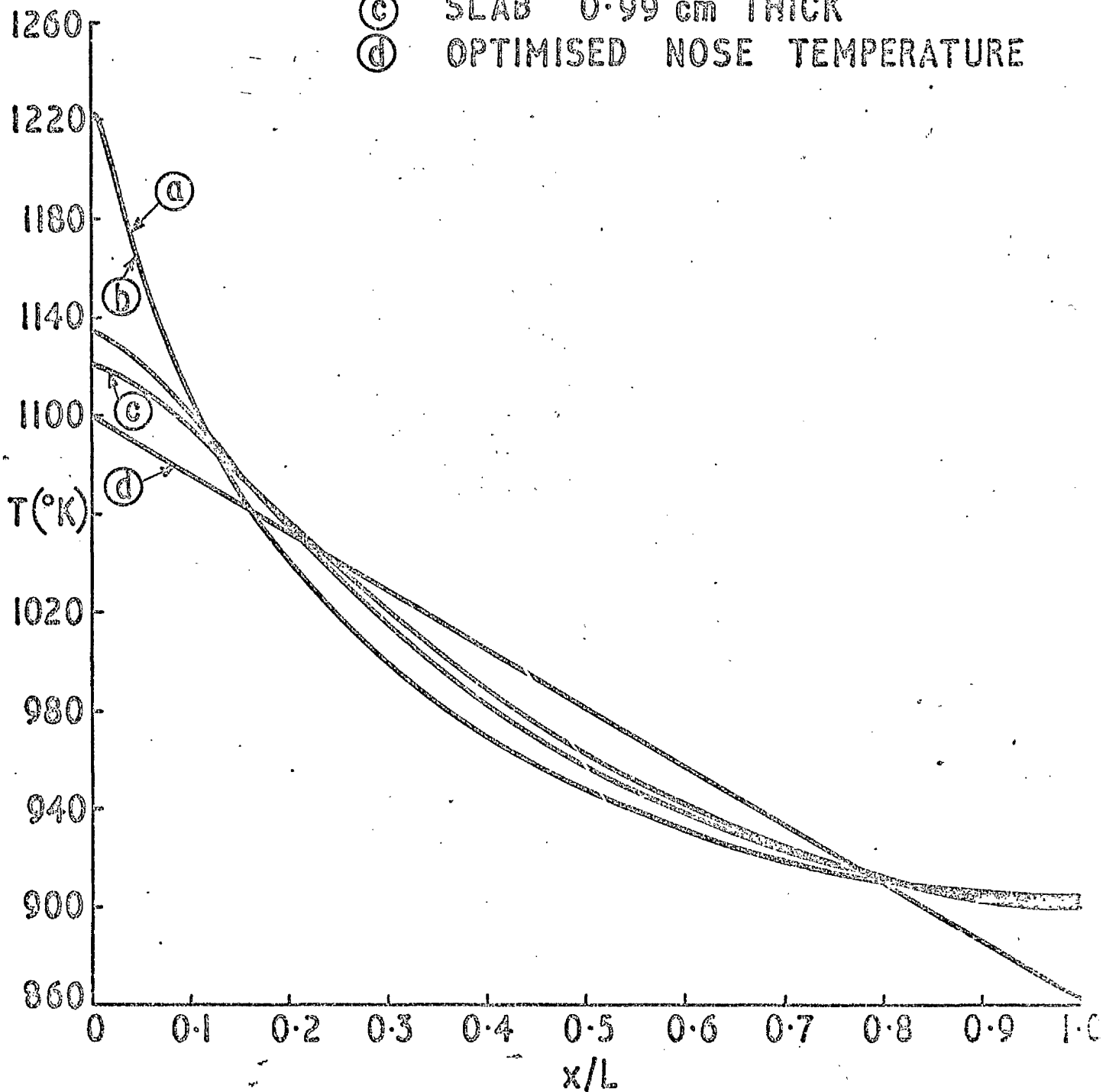
FIGURE 4.3.3

$$Q_0 = 10,000 \text{ W/m}^{3/2} \quad A = 15.04 \text{ cm}^2$$

$$\epsilon = 0.8 \quad k = 17.78 \text{ W/m } ^\circ\text{K}$$

$$L = 0.1524 \text{ cm}$$

- (a) WEDGE 1.956 cm END THICKNESS
- (b) TRAPEZOIDAL 0.66 - 1.321 cm
- (c) SLAB 0.99 cm THICK
- (d) OPTIMISED NOSE TEMPERATURE

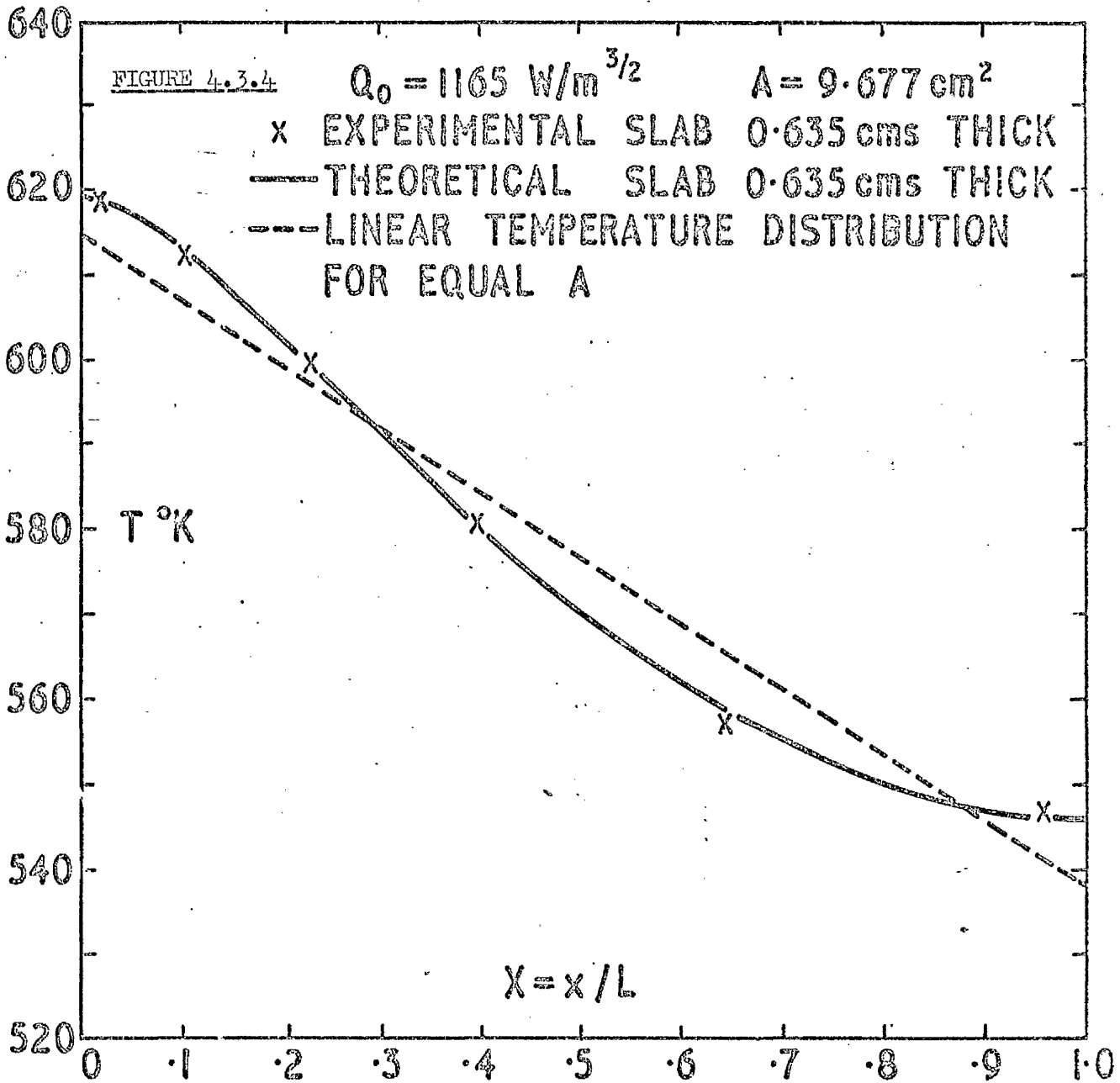


constants are identical (see Figure 4.3.1), we find that for a 5.8% increase in cross - sectional area, nose temperature decreases by only 1.5% and L must be increased by 17.5% to accommodate the optimisation. These considerations will be of practical use in designing a leading edge upon which no limitation of length has been placed.

It is convenient at this point to state that it is impossible to obtain an optimised shape if the values of length, L and cross - sectional area, A are fixed.

Comparisons between previously tested shapes e.g. those of Figures 2.1-3, are possible to some extent. A linear temperature distribution, which will not have a minimum value of nose temperature, can be calculated for cases where Q_0 , L and A are fixed; this can be done using equations 4.2.4 and 5. As an example, we will make a comparison with the model (a slab) of Figure 2.3. The result is shown in Figure 4.3.4. The nose temperature, which has not been minimised, falls by 4.2°K , compared to the slab, which represents a reduction of 0.7%. If the shape was an optimum then the reduction in nose temperature compared to a slab of the same area would be expected to be of the order of 2%.

After the calculation of the essential parameters such as T_0 , α , L or A equation 4.3 determines the product kt and hence the thickness of the leading edge. The shape, in general, has maximum thickness at 0.175 and the value is equal to twice the



average thickness of the leading edge. Equation 4.3 provides only the variation of material thickness and not the external leading edge shape which, allowing for the existence of interior cavities, may appear quite different.

4.4 Experimental Analysis of an Optimised Shape Leading Edge.

The experimental analysis was carried out to determine whether the theoretical analysis produced accurate results. Based on the theoretical analysis, a model was manufactured to represent a leading edge which would have an optimised shape; the model was constructed in such a way as to have one flat surface and the other surface following the thickness distribution provided by the theoretical analysis. The flat surface of the model was subjected to simulated aerodynamics heating corresponding approximately to $x^{-1/2}$ and is produced by the apparatus of reference 9. The model was tested, under vacuum, in exactly the same manner as the test models of Chapter 3, including placing the nose of the model at $x = x_0$ instead of $x = 0$.

4.4.1 Test Model.

As has already been stated (3.3.2) the size of the test model is limited, by the experimental apparatus, to $0.3048 \times 0.1524 \text{ m.}^2$. The length, L , being fixed at 0.1524 m. Since the thickness distribution of the leading edge is directly related to the value of the heat input constant, Q_0 (equation 4.3), the value of Q_0 should be taken as high as possible in order to maximise the thickness of the experimental model. The experimental apparatus was decided to be

capable of producing sufficient heat flux to allow $Q_0 = 1250 \text{ W/m}^{3/2}$ to be taken as a representative value of heat input constant.

The material chosen for the model was stainless steel, type F. C. B. Staybrite or A. I. S. I. - 347. This material was chosen since it had proved satisfactory in previous investigations. Its coefficient of thermal conductivity as given in 3.3.2 is $k = 15.9(1 + 0.00039 \times T^{\circ}\text{C}) \text{ W/m}^{\circ}\text{K}$ and its coefficient of emissivity can be taken as $\epsilon = 0.735(1 + 0.000297 \times T^{\circ}\text{C})$. To simplify and speed the calculation of the thickness distribution for the test model, it was decided to take average values of k and ϵ over the likely temperature range to which the model would be subjected. On this basis we used the figures $k = 17.78 \text{ W/m}^{\circ}\text{K}$ and $\epsilon = 0.8$ throughout the analysis.

Using these figures and the method of calculation described in 4.2, the optimised nose temperature, T_0 , was found to be 654.3°K , the cross-sectional area, A , of the model to be 3.1627 cm^2 and the linear temperature variation, α , across the model to be 922.5°K/m . The thickness distribution of the model was then found from equation 4.3. Table 4.4.1 shows the thickness distribution for the model and Figure 4.4.1(a) the shape of the model. The model has a thin tail and maximum thickness just greater than 0.4 cms. and since the nose and tail values of thickness are zero it can be seen that the model is particularly thin.

This thickness of test model caused serious difficulties during its manufacture; to overcome the problem of having a thin tail

Table 4.4.1. Thickness Distribution of the Experimental Model.

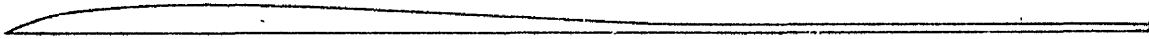
| <u>x (cms.)</u> | <u>kt (W / °K)</u> | <u>Theoretical Thickness (cms.)</u> | <u>Actual Thickness (cms.)</u> |
|-----------------|----------------------|---|------------------------------------|
| 0.000 | 0.000 | 0.0000 | 0.0000 |
| 0.7620 | 0.0519 | 0.2917 | 0.2917 |
| 1.5240 | 0.0708 | 0.3980 | 0.3980 |
| 2.286 | 0.0771 | 0.4338 | 0.4338 |
| 3.048 | 0.0771 | 0.4338 | 0.4338 |
| 3.81 | 0.0735 | 0.4133 | 0.4133 |
| 4.572 | 0.0678 | 0.3812 | 0.3812 |
| 5.334 | 0.0609 | 0.3428 | 0.3428 |
| 6.096 | 0.0536 | 0.3014 | 0.3014 |
| 6.858 | 0.0461 | 0.2593 | 0.2593 |
| 7.62 | 0.0388 | 0.2181 | 0.2181 |
| 8.382 | 0.0318 | 0.1790 | 0.1790 |
| 9.144 | 0.0254 | 0.1427 | 0.1427 |
| 9.906 | 0.0196 | 0.1100 | 0.127 |
| 10.668 | 0.0144 | 0.0811 | 0.127 |
| 11.43 | 0.0100 | 0.0565 | 0.127 |
| 12.192 | 0.0064 | 0.0361 | 0.127 |
| 12.954 | 0.0036 | 0.0203 | 0.127 |
| 13.716 | 0.0016 | 0.0090 | 0.127 |
| 14.478 | 0.0004 | 0.0022 | 0.127 |
| 15.24 | 0.0000 | 0.0000 | 0.127 |

FIGURE 4.4.1

(a) Shape of model as provided by theoretical analysis.



(b) Shape of experimental test model.



which tended to zero, the thickness of the model from approximately 0.75 of its length onwards was made constant at 0.127 cm. The shape of the model as it was actually tested is shown in Figure 4.4.1(b).

4.4.2 Experimental Procedure.

The experimental model was tested in exactly the same manner as the models of Chapter 3. The vacuum chamber apparatus did not require any modification.

The model is tested with its flat surface uppermost and exposed to thermal radiation from the reflector. The top surface is shot - blasted and blackened and has the co-efficient of emissivity stated in 4.4.1; the curved surface is highly polished using diamond powder and additional shielding against radiation heat loss is provided by placing a curved reflecting surface close to the polished surface of the model. The model rests on four ceramic pins.

Temperature measurements are taken at the middle section of the model by means of thermocouples which are spot - welded to the curved surface. The thermocouples are the same as those used in the experimental analysis of Chapter 3. Nine thermocouples were placed, in a single row, at prescribed locations along the curved surface. Although difficulties arose in model manufacture due to its thinness; one advantage arose out of this; if the model had been thicker, then because of its shape, it would be incorrect to assume that there is no temperature variation across the model thickness. The thermocouple e.m.f. was recorded in the same way

as in Chapter 3.

After the vacuum chamber had been evacuated, power to the reflector was steadily increased until the desired temperature conditions in the model were reached.

Table 4.4.2 gives the experimental results for the model and also provides a comparison with the theoretically predicted linear temperature variation.

The experimental errors encountered were the same as those of Chapter 3.

4.5 Discussion.

Figure 4.5.1 shows the experimental results for the model tested and compares them with the theoretical linear temperature variation.

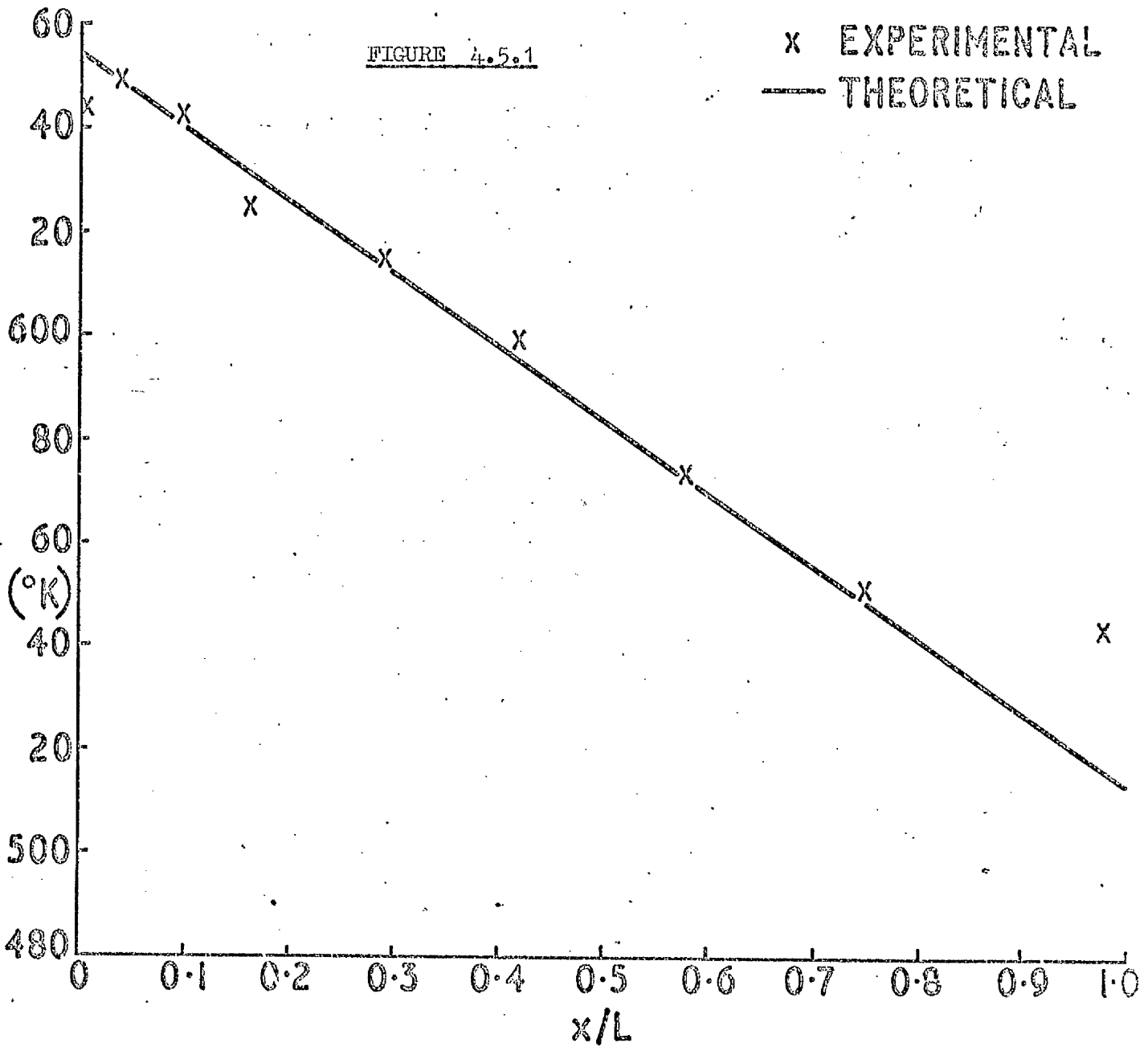
Considering the difficulties involved in manufacturing a model of this shape, the agreement between experiment and theory is exceptionally good. Excepting the first and last locations of temperature measurement, the difference between experiment and theory does not at any point exceed 0.9%.

The disagreement between experimental and theoretical results can be readily explained. The first thermocouple was placed as close as possible to the leading edge of the model in order to provide an, as accurate as possible, estimate of nose temperature.

Unfortunately the curved reflecting surface placed under the model could not extend completely to its leading edge, since, if it did, it would be subjected to heating, from the reflector, which, in turn,

Table 4.4.2.

| <u>$\frac{x}{L}$</u> | <u>Temperature ($^{\circ}\text{K}$)</u> | <u>Theoretical Temperature ($^{\circ}\text{K}$)</u> | <u>Percentage Difference</u> |
|---------------------------------|--|--|----------------------------------|
| 0.005 | 643.97 | 652.4 | - |
| 0.042 | 649.43 | 648.44 | 0.15 |
| 0.1 | 642.57 | 634.65 | 0.45 |
| 0.166 | 625.28 | 630.87 | 0.88 |
| 0.292 | 615.79 | 613.3 | 0.4 |
| 0.4166 | 599.44 | 595.72 | 0.63 |
| 0.5833 | 573.6 | 572.3 | 0.23 |
| 0.75 | 551.68 | 548.85 | 0.52 |
| 0.9792 | 542.98 | 516.63 | - |



would be transmitted to the curved surface of the model. Thus there is a certain amount of radiation heat loss at a small portion of the model, at the nose, which causes the reduction in temperature compared to theory.

The temperature measured at the last thermocouple location is higher than that predicted by theory due to the fact that the model thickness was made constant from 0.75 of its length onwards, to facilitate manufacture. Thus a greater amount of material was present at the tail than there would have been, had it been possible to manufacture the model exactly according to the theoretical thickness distribution. Consequently more heat flowed downstream into the tail than would have done for an exact model and so the temperature at the tail increased.

There is no practical value in calculating a value of Q_0 from the experimental results, since the calculated value would vary only slightly from the theoretical value due to the closeness of the experimental and theoretical results.

CHAPTER V.Conclusions and General Discussions.

In this study we have been concerned with two particular methods of reducing leading edge temperatures caused by aerodynamic heating during high speed flight. The study has been based on the theory of conducting plates which has been extended to cover our particular methods. The importance of the role of material thermal conductivity in moderating the leading edge temperature distribution has already been proved. The basis of our methods was to increase the conducting power of the leading edge; firstly, by increasing the thermal conductivity at the nose of the leading edge and secondly, by redistributing the material of the leading edge.

By employing a highly conducting nose bonded on to the main body, of lesser conducting material, of a leading edge, significant reduction in nose temperature is gained compared to a leading edge manufactured wholly of the lesser conducting material. The reduction in nose temperature increases with reducing amount of material present at the nose e.g. for a wedge, reduction in nose temperature is of the order of 10.5%, compared to a slab, 3.6% and a trapezoidal, 4.8%. Consequently it will now be possible to construct a sharp leading edge of highly conducting material or composite material which will produce the same nose temperature as a thicker leading edge of lower conductivity material.

By employing a highly conducting nose bonded on to the main body, of lesser conducting material, of a leading edge, significant reduction in nose temperature is gained compared to a leading edge manufactured wholly of the lesser conducting material. The reduction in nose temperature increases with reducing amount of material present at the nose e.g. for a wedge, reduction in nose temperature is of the order of 10.5%, compared to a slab, 3.6% and a trapezoidal, 4.8%. Consequently it will now be possible to construct a sharp leading edge of highly conducting material or composite material which will produce the same nose temperature as a thicker leading edge of lower conductivity material. There is only slight variation in the comparative reduction of nose temperature between a composite and lower conductivity leading edge with increased heating to the leading edge.

The experimental investigation concerning the composite leading edge proved the results predicted by the theory to be accurate; nowhere over the leading edge did the difference between experimental and theoretical results exceed 1.5%. This investigation also showed that the resistance to heat flow across the junction of the two materials was negligible. Thus the fear that a possible junction resistance to heat flow would reduce the benefits gained by employing a highly conducting nose was proved groundless.

Optimising the shape of the leading edge i.e. redistributing the material thickness available to give a minimum nose temperature

and linear temperature distribution over the leading edge, significantly reduces the nose temperature compared to other shapes of leading edge of the same cross - sectional area, e.g. comparing optimised shapes to slabs and trapezoidals we get reductions in nose temperature of 2% and 3% respectively; for a wedge the reduction varies slightly with heat input but never exceeds 11%. When calculating the important parameters, such as nose temperature, and then the optimised shape, either the value of cross - sectional area or length must be allowed to be variable. The value of cross - sectional area of the leading edge, when calculated on the basis of fixed length of leading edge, is directly linked to the value of Q_0 , the heat input constant. If both cross - sectional area and length of leading edge are fixed then a leading edge shape with minimised nose temperature cannot be obtained. However the leading edge thickness distribution can be re - arranged to give a linear temperature distribution over its length. This temperature linearisation produces a reduction in nose temperature, compared to a slab of the same cross - sectional area, of 0.7%; a fully optimised shape would expect to produce a reduction in nose temperature of the order of 2%.

The experimental investigation for the optimised shape proved the theory to be extremely accurate by producing exceptionally good agreement between experimental and theoretical results. The difference between experiment and theory did not

exceed 0.9%.

We will now compare the relative advantages of the two methods of reducing nose temperature which we have studied. Our basis for comparison will be the simple leading edge shapes - a slab, trapezoidal and wedge. Comparing composite leading edges of exactly the same dimensions as our three basic cases we get reductions in nose temperature of 3.6%, 4.8% and 10.5% respectively; comparing with the optimised shape leading edge we get reductions of 2%, 3% and 10.8% respectively.

The wedge shape is the closest approximation to a realistic leading edge shape and consequently more value can be attached to results gained from comparisons with wedge shapes. The fact that the reduction for wedge - optimised shape comparison is greater than the wedge - composite leading edge comparison is unimportant; what is important is that the values are almost equal. How then can we assess which method of nose temperature reduction is of the most practical value? The volume of material required to manufacture the leading edge will be an important factor; again using figures for the wedge comparison we find that the composite leading edge requires 18.6% less volume of material than the optimised shape leading edge to produce the same reduction in nose temperature. The problems involved in manufacturing leading edges based on our methods are considerable. During our experimentation concerning the composite leading edge, no study was undertaken to investigate whether any stresses were induced at the junction of the composing

materials due to a difference in coefficients of thermal expansion. No disturbances were apparent at the junction after our experimentation, but our heat input, even at its maximum, was unlikely to cause large expansions.

A leading edge based on optimised shape theory would have zero induced thermal stresses since the temperature distribution over its length is linear. The manufacture of such a leading edge would have to be to exceptionally high limits of accuracy, since any deviation from the theoretical thickness distribution would produce a non - linearity in the temperature distribution, which would result in the production of thermal stresses in a supposedly stress - free designed leading edge. Internal cavities in the leading edge would also produce difficulties.

Each method has its relative advantages and disadvantages and it is possible that a combination of both may provide a better solution than either separately.

Appendix A

Derivation of the Heat Conduction Equation in a Finite Differences Form.

To solve the heat conduction equation it is necessary to express it in a finite differences form. The heat conduction equation is expressed as

$$\frac{d}{dx} \left(kt \frac{dT}{dx} \right) = \epsilon \sigma T^4 - Q_0 / (x + x_0)^{\frac{1}{2}}$$

from equation 3.6. We have adopted the central difference notation for our analysis. The interval $x = 0, L$ is divided into N equal intervals with end points x_0, x_1, \dots, x_n , (where $x_0 = 0$ and $x_n = L$), where x_n at $n = 0$ is not to be confused with the constant x_0 , used to overcome the singularity at the leading edge for the laminar heat transfer expression. If we denote the value of temperature at x_n by T_n then equation 3.6 can be re-written (using reference 16) in the form

$$\frac{1}{h} [kt_{n+\frac{1}{2}} (T_{n+1} - T_n)] - \frac{1}{h} [kt_{n-\frac{1}{2}} (T_n - T_{n-1})] = h \left\{ \epsilon \sigma T_n^4 - \frac{Q_0}{(x_n + x_0)^{\frac{1}{2}}} \right\} \quad A.1$$

with $h = L / N$.

On re-arranging we get

$$kt_{n+\frac{1}{2}} T_{n+1} - (kt_{n+\frac{1}{2}} + kt_{n-\frac{1}{2}}) T_n + kt_{n-\frac{1}{2}} T_{n-1} = h \left\{ \epsilon \sigma T_n^4 - \frac{Q_0}{(x_n + x_0)^{\frac{1}{2}}} \right\} \quad A.2$$

i.e.

$$kt_{n+\frac{1}{2}} T_{n+1} - (kt_{n+\frac{1}{2}} + kt_{n-\frac{1}{2}} + h^2 \epsilon_n \sigma_n^3) T_n + kt_{n-\frac{1}{2}} T_{n-1} \\ = -h^2 \frac{Q_0}{(x_n + x_0)^2} \quad \text{where } n = 0(1)N \quad \text{A.3}$$

Equation A.3 represents $(N + 1)$ simultaneous equations with $N + 3$ unknowns, namely, $T_{-1}, T_0, T_1, \dots, T_n, \dots, T_N, T_{N+1}$. The values of T_{-1} and T_{N+1} occurring in the equation at $n = 0$ and $n = N$ respectively do not exist. However the boundary conditions at $x = 0, L$ supply us with the two additional relationships necessary. We know

$$\frac{dT}{dx} = 0 \quad \text{at } x = 0, L. \quad \text{A.4}$$

and in the present notation these can be expressed as

$$T_{-1} = T_1 \quad \text{and} \quad T_{N+1} = T_{N-1} \quad \text{A.5}$$

However equations A.3 are not a set of linear equations; but there may exist a convergent iterative method of solution. If $T_n^{(i)}$ denotes the value of T_n after the completion of the i^{th} iteration ($T_n^{(0)}$ being a starting value), then

$$[T_n^{(i+1)}]^4 = [T_n^{(i)} + (T_n^{(i+1)} - T_n^{(i)})]^4$$

and expanding

$$[T_n^{(i+1)}]^4 = T_n^{(i)4} + 4 T_n^{(i)3} [T_n^{(i+1)} - T_n^{(i)}] + R \quad A.6$$

where R is small if the difference between the interpolates is small. Thus we can re-write equation A.3 as

$$\begin{aligned} kt_{n+\frac{1}{2}} T_{n+1}^{(i-1)} + kt_{n-\frac{1}{2}} T_{n-1}^{(i)} - [kt_{n+\frac{1}{2}} + kt_{n-\frac{1}{2}} + 4h^2 \epsilon_n \sigma T_n^{(i-1)3}] T_n^{(i)} \\ = -h^2 \left\{ \frac{Q_0}{(x_n + x_0)^2} + 3 \epsilon_n \sigma T_n^{(i-1)4} \right\} \end{aligned} \quad A.7$$

Equation A.7 can be more concisely represented by the matrix equation

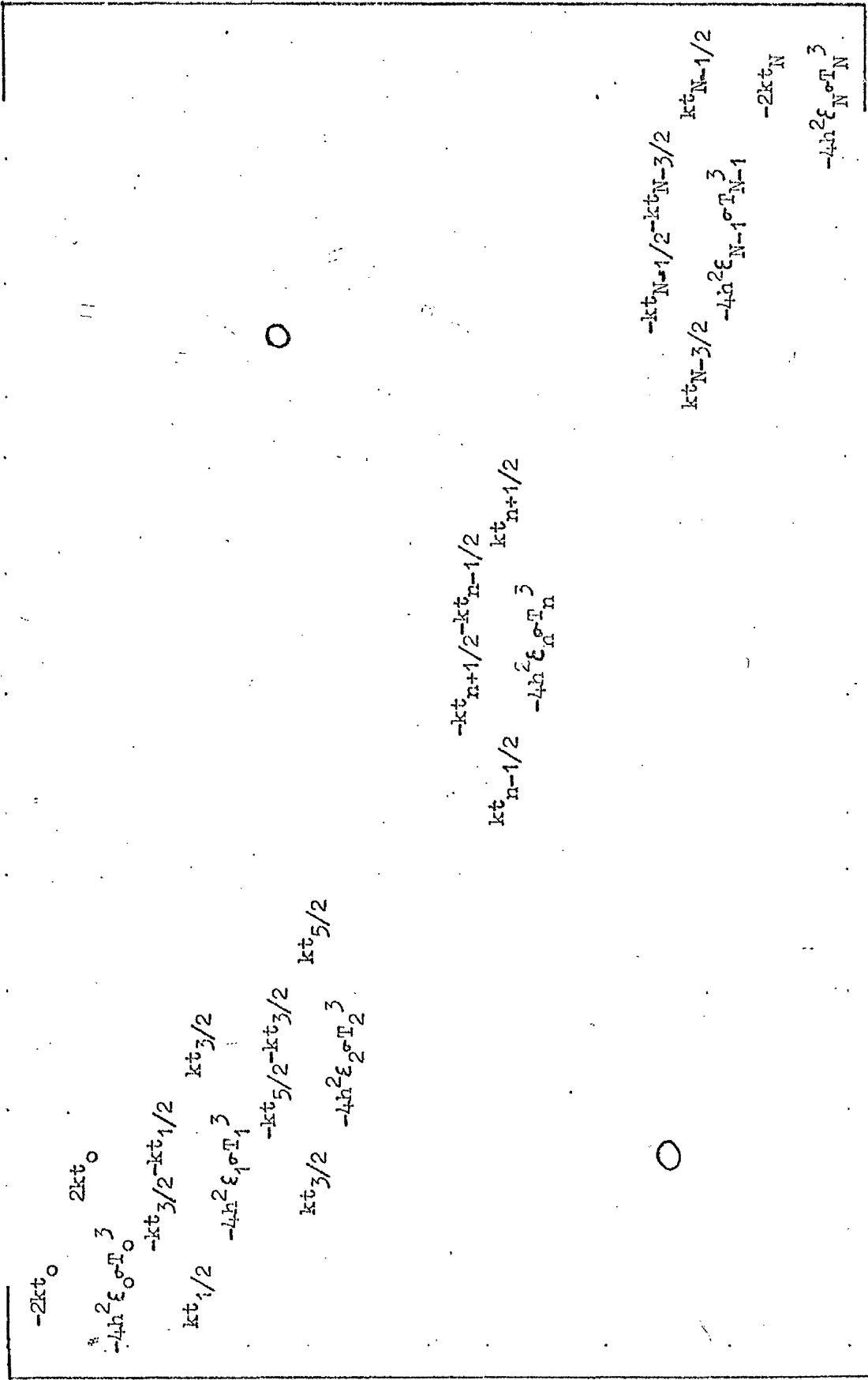
$$\underline{C} \cdot \underline{T} = \underline{B} \quad A.8$$

where \underline{T} is the vector $(T_0, T_1, T_2, \dots, T_n, \dots, T_N)$; \underline{B} is the column vector whose general element is $-h^2 \left\{ \frac{Q_0}{(x_n + x_0)^2} + 3 \epsilon_n \sigma T_n^{(i)4} \right\}$ and \underline{C} is the band matrix shown overleaf.

Under the specified boundary conditions (equations A.4. or A.5) for $n = 0$ and $n = N$, the following relations have been used in the matrix \underline{C} .

$$\text{and } \left. \begin{aligned} kt_{\frac{1}{2}} &= kt_{-\frac{1}{2}} \\ kt_{N+\frac{1}{2}} &= kt_{N-\frac{1}{2}} \end{aligned} \right\} \quad A.9$$

Also for sufficiently small values of h,



$$-2kt_0$$

$$-4h^2 \epsilon_0 \sigma_0^3$$

$$2kt_0$$

$$-kt_3/2 - kt_1/2$$

$$kt_3/2$$

$$kt_1/2$$

$$-4h^2 \epsilon_1 \sigma_1^3$$

$$-kt_5/2 - kt_3/2$$

$$kt_5/2$$

$$kt_3/2$$

$$-4h^2 \epsilon_2 \sigma_2^3$$

$$-kt_{n+1}/2 - kt_n - 1/2$$

$$kt_{n-1}/2$$

$$-4h^2 \epsilon_n \sigma_n^3$$

$$kt_{n+1}/2$$

$$-kt_{N+1}/2 - kt_N - 3/2$$

$$kt_N - 3/2$$

$$kt_{N-1}/2$$

$$-4h^2 \epsilon_{N-1} \sigma_{N-1}^3$$

$$-2kt_N$$

$$-4h^2 \epsilon_N \sigma_N^3$$

$\sigma =$

$$\left. \begin{array}{l} kt_{\frac{1}{2}} + kt_{-\frac{1}{2}} \approx 2kt_0 \\ \text{and } kt_{N+\frac{1}{2}} + kt_{N-\frac{1}{2}} \approx 2kt_N \end{array} \right\} \text{A.10}$$

are valid approximations.

We can write

$$\underline{C}^{(i-1)} \cdot \underline{T}^{(i)} = \underline{B}^{(i-1)} \quad \text{A.11}$$

to represent that $T_n = T_n^{(i-1)}$ is used in the elements of \underline{C} and \underline{B} whilst solving for $T_n^{(i)}$.

Appendix B

ALGOL - 60 Computer Program

B.1 Description of the Computer Program. The input of data is done with the aid of the procedure " RW ". All quantities in the program are non-dimensionalised with respect to the leading edge length, L, thermal conductivity at 0°C for steel, designated as k0(2) and the Stefan - Boltzman constant, σ , which gives a reference temperature for steel of $TR(2) = \left(\frac{k0(2)}{\sigma \times L} \right)^{\frac{1}{3}}$. The reference temperature for copper, TR(1), is calculated, for comparison, using k0(1).

The leading edge is divided into a grid in the chordwise direction. N gives the number of grid points. A constant value of temperature is then assigned to every element of the array < T >. Execution of the main program starts with a call on the procedure " Tempdist ".

Procedure " assign ", incorporating procedures kt, Q, and emissivity assigns values, according to the values of temperature in the array < T >, to the procedure " bandsolve " which calculates new temperature values for the array < T >. This process is continued until the criterion for convergence between two consecutive solutions is satisfied. If the solutions do not converge after a specified number of iterations, program control is switched to the label UNCON. After a converged solution of the equation is obtained, the grid size, N is doubled, and the solution for this value of N is compared to the

previous solution for one-half the grid size. This doubling continues until this so-called discretisation criterion is satisfied. If too large a grid size is required then program control is switched to label DISCRETE.

On successful completion of the program the output consists of the data followed by the reference temperatures, grid size and the temperature distribution tabulated against the distance from the leading edge.

B.2. The following is the text of a working ALGOL computer program reproduced directly from paper tape. It starts on the first line of the next page.

begin

comment SOLVES THE ONE-DIMENSIONAL HEAT CONDUCTION

EQUATION FOR A COMPOSITE MATERIAL HYPERSONIC WING.

BANDSOLVE, AN ITERATIVE PROCESS IS EMPLOYED TO

SOLVE THE EQUATION IN THE FINITE DIFFERENCES FORM.

Procedure bandsolve solves the N+1 non-homogeneous

non-linear set of simultaneous equations at each

iteration. The process of iteration is repeated

until the solution lies within some permissible

error eps. Bandsolve avoids the storage of

unnecessary zeros by reducing the size of the

matrix <c> from [0:N,0:N] to [-1:1,0:N];

comment The thermal conductivity, surface emissivity

and the thickness of the material can all be

functions of temperature and position. In the

particular non-dimensional system used, the basic

parameters used are k0[1] and k0[2] at T = 0 DEGK,

sigma and length,L together with reference

temperatures TR[1] = (k0[1]/sigma*L)^{1/3} for

copper and TR[2] = (k0[2]/sigma*L)^{1/3} for steel;

real procedure RW(S); string S;

begin

real t;

RW:=t:=read (20); write text (70,S); space (70,3);

```

output(70,t);  newline (70,1);
end  RW;
real procedure kt (T,x);  value x,T;  real T,x;
  comment provides the product of thermal
    conductivity and the thickness of the model. k
    and t can both be functions of temperature and x,
    the distance from the leading edge, but not
    necessarily so;
  begin
    comment uses non-local array data;
    if x < data[12] then
      kt:=(k0[1]/k0[2])*(1+data[5]*(T-273.15/TR[2]))
        *(data[3]+data[4]*x)  else
      kt:=(1+data[9]*(T-273.15/TR[2]))*(data[3]+data[4]*x);
    end  kt;
real procedure Q(T,x);  value x,T;  real T,x;
  comment provides the heat input to the model. Q
    being a function of T and x;
  begin
    comment uses non-local variables Q0 and x0;
    Q:=Q0/sqrt(x+x0);
  end  Q;
real procedure emissivity(T,x);  value T,x;  real T,x;
  comment provides the variation of emissivity with
    temperature and position;

```

```

begin
comment uses non-local array data;
if x < data[12] then
    emissivity:=data[7]*(1+data[8]*(T-273.15/TR[2])) else
    emissivity:=data[10]*(1+data[11]*(T-273.15/TR[2]));
end emissivity;
procedure TempDist (N,T,UNCON,FAIL,DISCRETE);
integer N; label UNCON,DISCRETE,FAIL; array T;
comment The array <T> is assigned starting values
before entry into TempDist. Either these values
can all be some constant or a fraction of the
local radiation equilibrium temperature. The
latter method would require some rootsolve
procedure. The one-dimensional heat conduction
equation is solved using the method of finite
differences. N+1 simultaneous non-homogeneous and
non-linear equations have to be solved for N+1
unknowns. In any one equation most of the terms
are zero (maximum of three non-zero terms) and
Gaussian Elimination is employed inside the
procedure bandsolve to overcome the objection of
profligate storage. The interval over which the
integration is carried out is divided into N
equal intervals, each one being  $h=1/N$  where the
entire length is  $x=1$ . The accuracy of the

```

iterative solution is controlled by the product of ϵ and $N+1$. Integer M supplies the limit on the maximum number of iterations to be attempted. This is to safeguard against either an instability in the set of equations or the starting values of the array $\langle T \rangle$ to be such as to cause a divergence in the solution. In case of an unconverged solution, control is switched to the label UNCON. The label FAIL is an outlet from the procedure bandsolve in case the set of equations has a singularity. The label DISCRETE provides an outlet from the program if too large a number of internal points are demanded to satisfy the discretisation error. Upon normal completion the solution is stored in the array $\langle T \rangle$;

comment uses non-local real procedures kt,Q and emissivity;

begin

procedure bandsolve (c,x,b,N,FAIL); value N;

integer N; array b,c,x; label FAIL;

comment solves the system of linear equations

represented by $c[-1,k]x[k-1] + c[0,k]x[k] + c[1,k]x[k+1] = b[k]$, for $k=0(1)N$, where $c[-1,0]$ and $c[1,N]$ do not exist (i.e. vanish identically). If the system is singular control is transferred to label FAIL, else

```

values are assigned to x[0],.....x[N];
comment actual arrays corresponding to formals
b and x to be defined for subscript limits
[0:N] and that corresponding to c for [-1:1,0:N];
begin
real a,d,eps;
integer k;
eps:=N/2↑37; d:=c[0,0];
if d=0 then goto FAIL;
for k := 1 step 1 until N do
    begin
        a:=c[-1,k]/d; b[k]:=b[k]-a×b[k-1];
        d:=c[0,k]-a×c[1,k-1];
        if abs (d)<abs (c[0,k])×eps then
            goto FAIL else c[0,k]:=d;
        end Gaussian elimination;
    x[N]:=b[N]/d;
    for k := N-1 step -1 until 0 do
        x[k]:=(b[k]-c[1,k]×x[k+1])/c[0,k];
    end bandsolve;
procedure assign(N,h,c,b,T); value N,h;
integer N; real h; array c,b,T;
comment After each iteration the values of the
terms in the arrays <c> and <b> are updated
here using the values of the temperatures

```

```

stored in the array <T>;
begin
integer k;
real a,d,f;
r:=4.0xhxh;
for k := N-1 step -1 until 1 do
    begin
        c[-1,k]:=a:=kt(0.5x(T[k]+T[k-1]),hx(k-0.5));
        c[1,k]:=d:=kt(0.5x(T[k]+T[k+1]),hx(k+0.5));
        c[0,k]:=- (a+d+fmissivity(T[k],kxh)xT[k]^3.0);
        end ;
    c[1,0]:=a:=2xkt(T[0],0);
    c[0,0]:=- (a+fmissivity(T[0],0)xT[0]^3.0);
    c[-1,N]:=a:=2xkt(T[N],Nxh);
    c[0,N]:=- (a+fmissivity(T[N],Nxh)xT[N]^3.0);
    for k := 0 step 1 until N do
        begin
            b[k]:=-hxh x(Q(T[k],kxh)
                +3xmissivity(T[k],kxh)xT[k]^4.0);
        end ;
    end assign;
integer m,j,k;
real term,eps,sum;
array Tcopy,TCHECK,b[0:960],c[-1:1,0:960];
comment The value of N is doubled everytime a

```

converged solution of the equation is obtained until the sum of the discretisation errors between the converged solution with twice the grid points and one with only half the points are of the same order as the convergence error. Data[2] supplies the error control on both these loops. The doubling process is allowed 7 times - making N equal to 960. If a converged solution is obtained before N= 7 then the program jumps to label CARRYON, otherwise control is switched onto the label DISCRETE;

```

for j := 1 step 1 until 7 do
  begin
    h:=1/N; term:=-data[2]×(N÷2+1); eps:=-data[2]×(N+1);
    for m := 1 step 1 until 100 do
      begin
        sum:=eps;
        for k := 0 step 1 until N do TCOPY[k]:=T[k];
        assign(N,h,c,b,T); bandsolve(c,T,b,N,FAIL);
        for k := 0 step 1 until N do
          sum:=sum+abs(TCOPY[k]-T[k]);
        if sum<0 then goto RETURN;
        end ;
        goto UNCON;
      RETURN: if j=1 then goto JUMP;

```

```

    for k := N+2 step -1 until 0 do
        term:=term+abs(TCHECK[k]-T[k+k]);
    if term<0 then goto CARRYON;
    if j=7 then goto DISCRETE;
JUMP: for k := 0 step 1 until N do TCHECK[k]:=T[k];
    N:=N+N;
    comment The new terms introduced into the
        array <T> upon doubling <N> are assigned
        values by interpolating midway between the
        existing terms of array <T>;
    for k := N+2 step -1 until 0 do T[k+k]:=T[k];
    for k := 1 step 2 until N do
        T[k:=(T[k-1]+T[k+1])/2.0;
    end ;

```

CARRYON:

```

    end TempDist;
    integer N,k,f1,f2,f3,ordinate;
    real L,Q0,x0,SIGMA,ROOTL,h;
    array data[1:15],T[0:960],TR,k0[1:2];
    boolean MORE;
    open(20); open(70);
    write text (70,[[c]MURRAY*STEELE***AERO*ENG.[3c]
        TEMPERATURE*DISTRIBUTION*FOR*ONE-DIMENSIONAL*HEAT*
        FLOW*AT*THE*LEADING*EDGE*OF*A*HYPERSONIC*WING[2c]
        USING*THE*METHOD*OF*FINITE*DIFFERENCES]);

```

```

SIGMA:=5.6710-8;
comment Sigma has units in Watts-metres-Degk;
f1:=format ([4s-ndd.ddd]); f2:=format ([10s-ndddd.de]);
f3:=format([10s-nd.dddde]);
LOOP: write text(70,[[p]]);
kO[1]:=RW([THERMAL*CONDUCTIVITY*OF*COPPER*AT*O*DEG*
CENTIGRADE*-*UNITS**WATTS/METRE.DEGK]);
kO[2]:=RW([THERMAL*CONDUCTIVITY*OF*STEEL*AT*O*DEG*
CENTIGRADE*-*UNITS**WATTS/METRE.DEGK]);
L:=RW([CHORD*LENGTH*IN*METRES]);
TR[1]:=(kO[1]/SIGMA/L)1/3.0;
TR[2]:=(kO[2]/SIGMA/L)1/3.0; xO:=RW([NON-DIMENSIONAL*XO]);
ROOTL:=sqrt(L);
QO:=RW([HEAT*FLUX*AT*NOSE*-*UNITS**WATTS/METRE1/3/2])
×ROOTL/kO[2]/TR[2];
data[6]:=L×100.0;
data [1]:=RW([STARTING*VALUE*OF*TEMPERATURE])/TR[2];
data[2]:=RW([TOLERANCE*ON*SUCCESSIVE*ITERATIONS*AND*
DISCRETISATION*ERROR]);
data[3]:=RW([MODEL*NOSE*THICKNESS*-*UNITS*-*
CENTIMETRES])/data[6];
data[4]:=RW([MODEL*TAIL*THICKNESS*-*UNITS*-*
CENTIMETRES])/data[6];
data[5]:=RW([CO-EFFICIENT*OF*THERMAL*CONDUCTIVITY*OF*
COPPER*-*ALPHA*-*UNITS*PER*DEGC])×TR[2];

```

```

data[9]:=RW([CO-EFFICIENT*OF*THERMAL*CONDUCTIVITY*OF*
  STEEL*--*ALPHA*--*units*PER*DEGC])×TR[2];
data[7]:=RW([EMISSION*OF*COPPER*AT*0*DEGC]);
data[10]:=RW([EMISSION*OF*STEEL*AT*0*DEGC]);
data[8]:=RW([THERMAL*VARIATION*OF*EMISSION*OF*
  COPPER*--*UNITS*--*PER*DEGC])×TR[2];
data[11]:=RW([THERMAL*VARIATION*OF*EMISSION*OF*
  STEEL*--*UNITS*--*PER*DEGC])×TR[2];
data[12]:=RW([LENGTH*OF*COPPER*NOSE*--*UNITS*--*
  CENTIMETRES])/data[6];
data[4]:=(data[4]-data[3]);
write text (70,[REFERANCE*TEMPERATURES*DEGC*==*]);
write (70,format([-ndddd.dcc]),TR[1]); write text (70,[AND]);
write (70,format([-ndddd.dcc]),TR[2]); newline (70,6);
N:=15; MORE:=read boolean (20);
for k := 0 step 1 until N do T[k]:=data[1];
comment data[1] supplies a constant starting value
  which has been assigned to every term of array <T>;
TempDist(N,T,UNCON,FAIL,DISCRETE);
write text (70,[NUMBER*OF*INTERVALS*--*GRID*SIZE*==*]);
write(70,format([-ndddd]),N); newline(70,2);
write text (70,[CENTIMETRES*FROM*NOSE***TEMPERATURE*DEGC]);
newline (70,1); h:=hxdata[6];
for k := 0 step 1 until N do
  begin

```

```
write (70,f1,k×h); write (70,f2,T[k]×TR[2]);
```

```
end ;
```

```
goto if MORE then LOOP else FINISH;
```

```
FAIL: write text(70,[_SINGULARITY*ENCOUNTERED_]);
```

```
DISCRETE:
```

```
write text(70,[_DISCRETE*ERROR*TOO*LARGE_]);
```

```
UNCON: write text(70,[_SOLUTION*NOT*CONVERGED_]);
```

```
if MORE then goto LOOP;
```

```
FINISH: close (20); close (70);
```

```
comment Data (15, boolean);
```

```
end→
```

B.3 The input to the computer program consists of a set of 16 parameters followed by a boolean statement. If the boolean is declared true then the program expects to read another set of data; if false then the program is terminated.

REFERENCES

- | <u>No</u> | <u>Author</u> | <u>Titles et .</u> |
|-----------|--|---|
| 1. | Silverstein C.C. | A Feasibility Study of Heat-Pipe-Cooled Leading Edges for Hypersonic Cruise Aircraft NASA GR-1857, November, 197. |
| 2. | Nonweiler T.R.F. | Surface Conduction of the Heat Transferred from a Boundary Layer. CoA Report No.59, 1952. |
| 3. | Nonweiler T.R.F. | Aerodynamic Problems of Space Vehicles . J.R.Ae.Soc 63(585), 1959. |
| 4. | Naysmith A. Woodley J.G. | Equilibrium Temperatures on Lifting Surfaces at Mach Numbers between 5 and 12 at altitudes from 80,000 ft. up to 15,000 ft. R.A.E. TR 67114, May, 1967. |
| 5. | Capey E.C. | Alleviation of Leading Edge Heating by Conduction and Radiation. R.A.E. Tech.Note No. 66311, October, 1966. |
| 6. | Nonweiler T.R.F. Wong H.Y. Aggarwal S.R. | The Role of Heat Conduction in Leading Edge Heating - Theory and Experiment. Glasgow University Report No. 6901, June, 1969. Also Aeronautical Research Council ARC Report No.31445, HYP 775 Also ARC CP No.1126. |
| 7. | Nonweiler T.R.F. Wong H.Y. Aggarwal S.R. | The Role of Heat Conduction in Leading Edge Heating. Presented at EUROMECH-20 held at Cambridge, July, 1970. Also Ingenieur Archiv. |

- | <u>No</u> | <u>Author</u> | <u>Titles etc.</u> |
|-----------|----------------------------|---|
| 8. | Sinha B.P. | Conduction of Heat wit' in a Body subjected to Aerodynamic Heating at Hypersonic Speeds. Ph.D.Thesis, University of Glasgow, September, 1966. |
| 9. | Wong H.Y. Sinha B.P. | Design of an Infra-Red Radiation Reflector for simulating Aerodynamic Heating at Hypersonic Speeds. Aeronautical Research Council Report No. 29218, 1967. |
| 10. | Aggarwal S.R. | The Role of Heat Conduction at the Leading Edge of a Hypersonic Wing. Ph.D. Thesis, University of Glasgow, January, 1971. |
| 11. | Wong H.Y. Aggarwal S.R. | Radiometer for measuring Thermal Radiation of One-Dimensional Intensity. Laboratory Practice, Oct. 1968. |
| 12. | Firth - Vickers. | Stainless Steel Ltd., Technical Data Sheet No. 108/17. |
| 13. | Touloukian Y.S. | Thermophysical Properties of High Temperature Solid Materials. The Macmillan Company, Vol.I, 1965. |
| 14. | Wong H.Y. Aggarwal S.R. | Measurement of Total Hemispherical Emittance. Laboratory Practice Jan. 1969. |
| 15. | Jacob M. | Heat Transfer. Vol.I, Chapman & Hall Ltd., 1959. |
| 16. | Collatz L. | The Numerical Treatment of Differential Equations. Springer - Verlag, 1960. |
| 17. | Lanczos C. | The Variational Principles of Mechanics (Chapter II). University of Toronto Press, 1966. |

UNIVERSITY OF GLASGOW

In respect of my thesis [title to be inserted]

"Reduction of leading edge temperatures during high speed flight".

1. I understand that no access to it will be allowed without my prior permission until one year has elapsed from the date of its deposit in the University Library.

2. Thereafter:-

* a. I give permission for it to be made available to readers in the University Library or within another library.

~~* b. I do not wish it to be made available to readers for a further two years without my written consent or (failing a reply from me within 3 months to a request from the University Library) the consent of the Library Committee in consultation with the Higher Degrees Committee of the Faculty.~~

3. Once any restrictions on access have expired:-

a. I give permission for a photocopy to be made by the British Library for lending to other libraries.

~~b. I * give/do not give permission for the University Library to make photocopies for other libraries or individuals without my specific authorisation. Note : Any prohibition on photocopying will lapse after five years from the date of deposit.~~

Signed *W. M. B. Steele*

Date *10/3/76*

* Strike out the sentence or phrase which does not apply.

Mr. William Steele - Thesis 3897 - 1973

Engineering

SUMMARY

It has already been shown that by taking into consideration the conducting power of the leading edge material, nose temperatures are substantially reduced compared to the case where aerodynamic heating is balanced by radiation alone. The leading edge is envisaged as a "conducting plate" and the heat transfer equations formulated. This investigation is concerned with two particular methods of reducing leading edge temperatures by increasing the conducting power of the leading edge.

The first involves manufacturing a leading edge consisting of a basic structural material on to which is bonded a nose of highly conducting material. The main problem which arises is that a thermal resistance may be set up across the interface of the two structural materials and it is possible that the reduction gained in nose temperature will be offset by this thermal resistance. Steady state heat transfer equations are set up to allow for the variation in material properties. Experimentation is carried out to determine the junction thermal resistance, which cannot be obtained analytically, and to investigate the accuracy of the results predicted by the solution of the heat transfer equations. Models of simple shapes, are manufactured from copper and stainless steel to represent the leading edge and are subjected to simulated aerodynamic heating.

The object of the other part of the investigation is to find the material distribution for a leading edge such that it has

a minimum nose temperature for the amount of material available and a linear temperature distribution over its length. Previous investigations have been concerned mainly with relatively simple leading edge shapes. By taking the temperature distribution as linear a stress free leading edge is obtained and the analysis of the thickness distribution is considerably simplified since the heat transfer equation becomes directly integrable. A model was manufactured on the basis of the analysis and subjected to simulated aerodynamic heating to provide a comparison with the predicted results.